



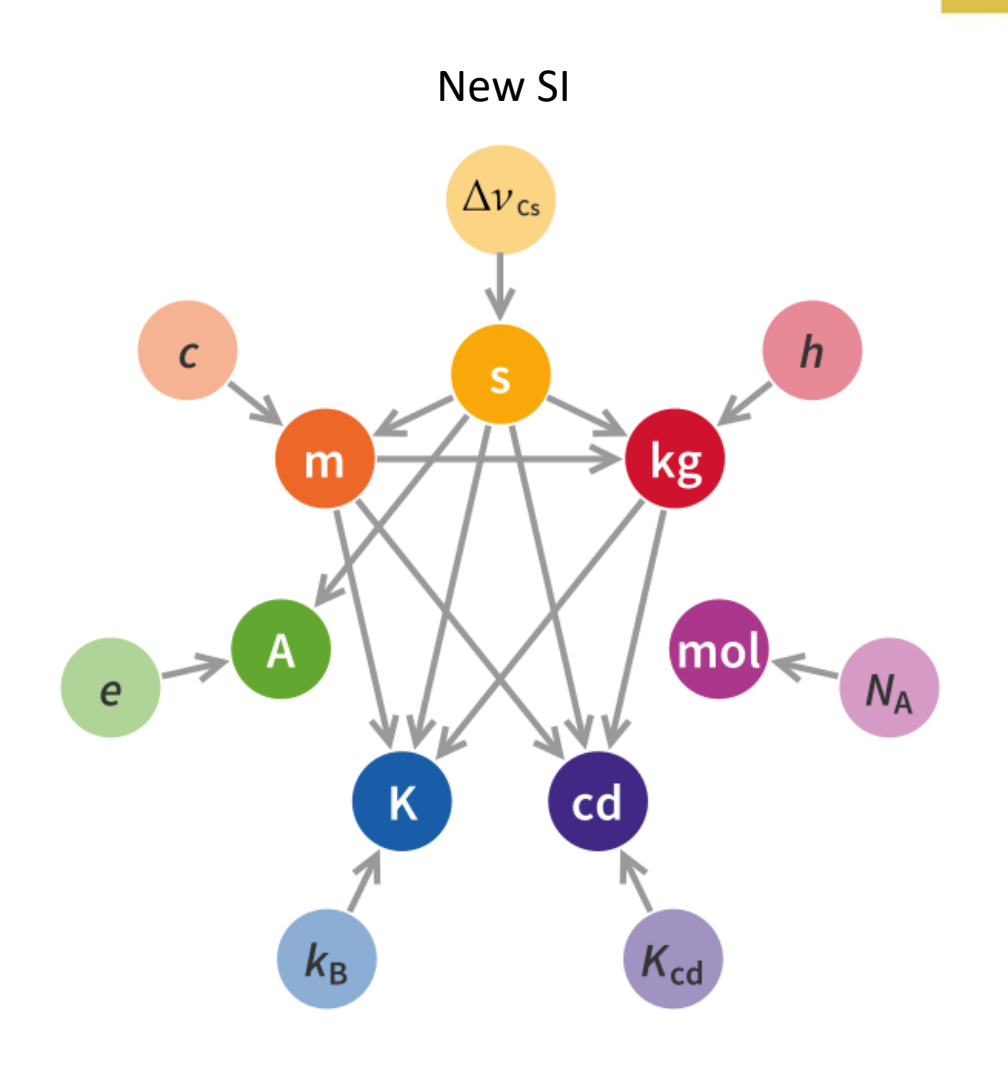
Programmable Cluster State with Josephson Metamaterials

Superconducting Devices for Quantum Optics ECT* - Trento 8 October 2025

Emanuele ENRICO (e.enrico@inrim.it)

INRiM - Introduction







INRiM - Divisions



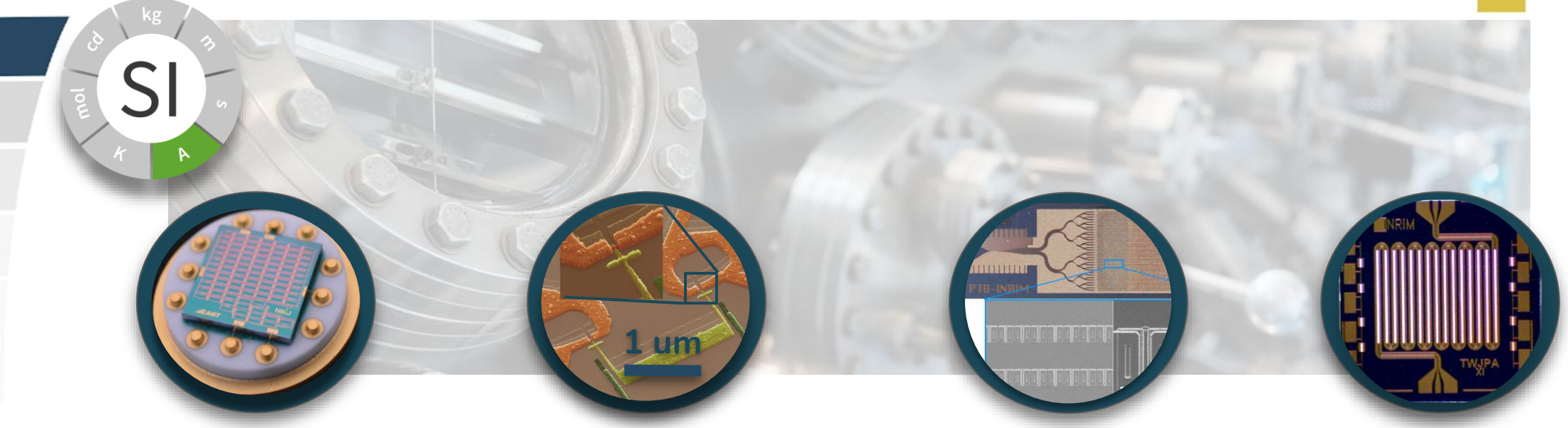
Advanced materials metrology and life science

Applied metrology and engineering

Quantum metrology and nano technologies



Quantum Electronics - NanoTech



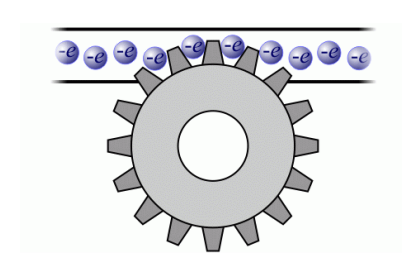
Quantum Hall Array Resistance Standard

 $R_{\rm H} = R_{\rm K}/i$

with $R_K = h/e^2$

and i = 1, 2, 3, 4, ...

Quantized-charge transport DC current standard



I=nef

Josephson Voltage Standard

 $V_J = n K_J f$

with $K_1 = h/2e$

and k = 1, 2, 3, 4, ...

Microwave photonics

v	1 GHz →20 GHz
<i>λ=c/v</i>	300 cm →15 cm
E=h/v	4 μeV→80 μeV
T=E/k _B	50 mK→1K



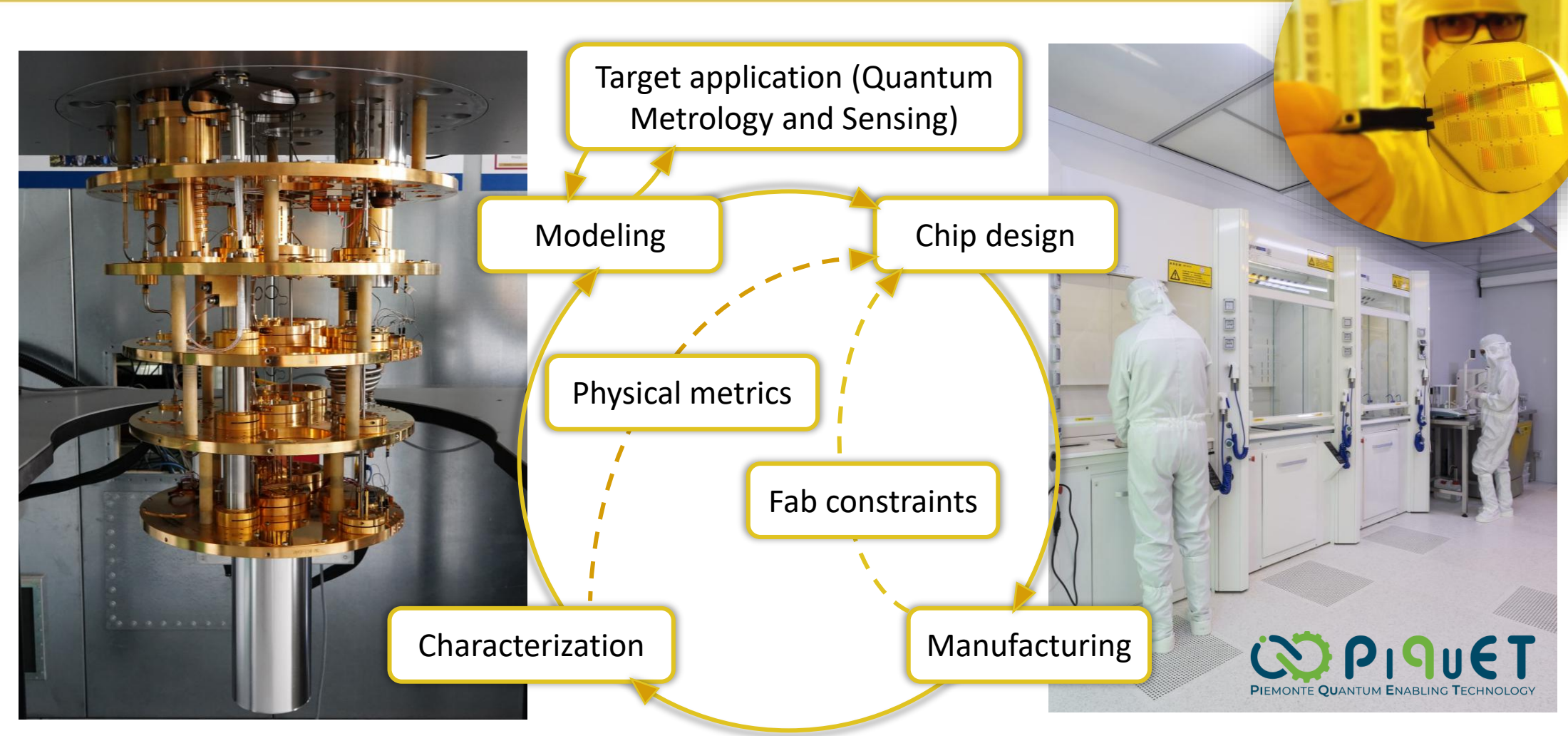
Superconducting Quantum Electronics



- Researchers
 - Emanuele ENRICO (PI)
 - Luca FASOLO
 - Luca OBERTO
 - Luca CALLEGARO
- PhD Students
 - Alessandro ALOCCO (PoliTO)
 - Andrea CELOTTO (PoliTO)
 - Emanuele PALUMBO (PoliTO)
 - Bernardo GALVANO (UniPA)
- Master/Bachelor students
 - Fabrizio BISOGNO (UniTO)
 - Tommaso SABBADINI (PoliTO)
- CleanRoom Technician
 - Start on July



Our workflow



Quantum Circuit for Metrology laboratory

hosting a dilution refrigerator (T < 20 mK)

PiQuET Cleanroom facility



Quantum Ciruits for Metrology Lab.



Dilution Refrigerator

- Leiden CF-CS110
- (400 μW @ 100 mK, BT < 20 mK)
- Warm insertable probe for RF
- μMetal(RT) and CryoPhy(BT) shields
- Warm insertable probe for QHE
- 9T magnet option

Shielded and thermally stable room

- Control electronics (DC+RF)
- CW (PNA-X) and pulsed protocols (QCS)



Superconducting Devices for Quantum Optics

(with a metrological flavor)



SPDC and Metrology – Quantum Adv.

nature photonics

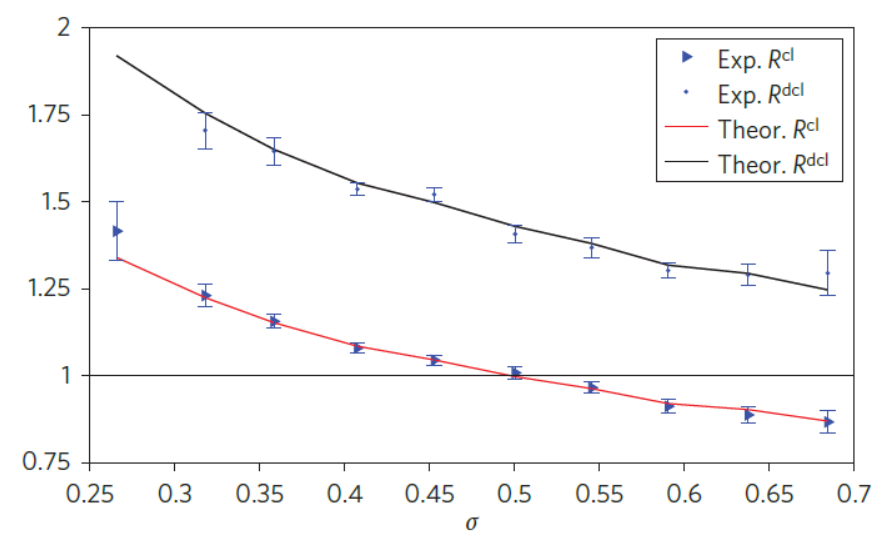
LETTERS

PUBLISHED ONLINE: 28 FEBRUARY 2010 | DOI: 10.1038/NPHOTON.2010.29

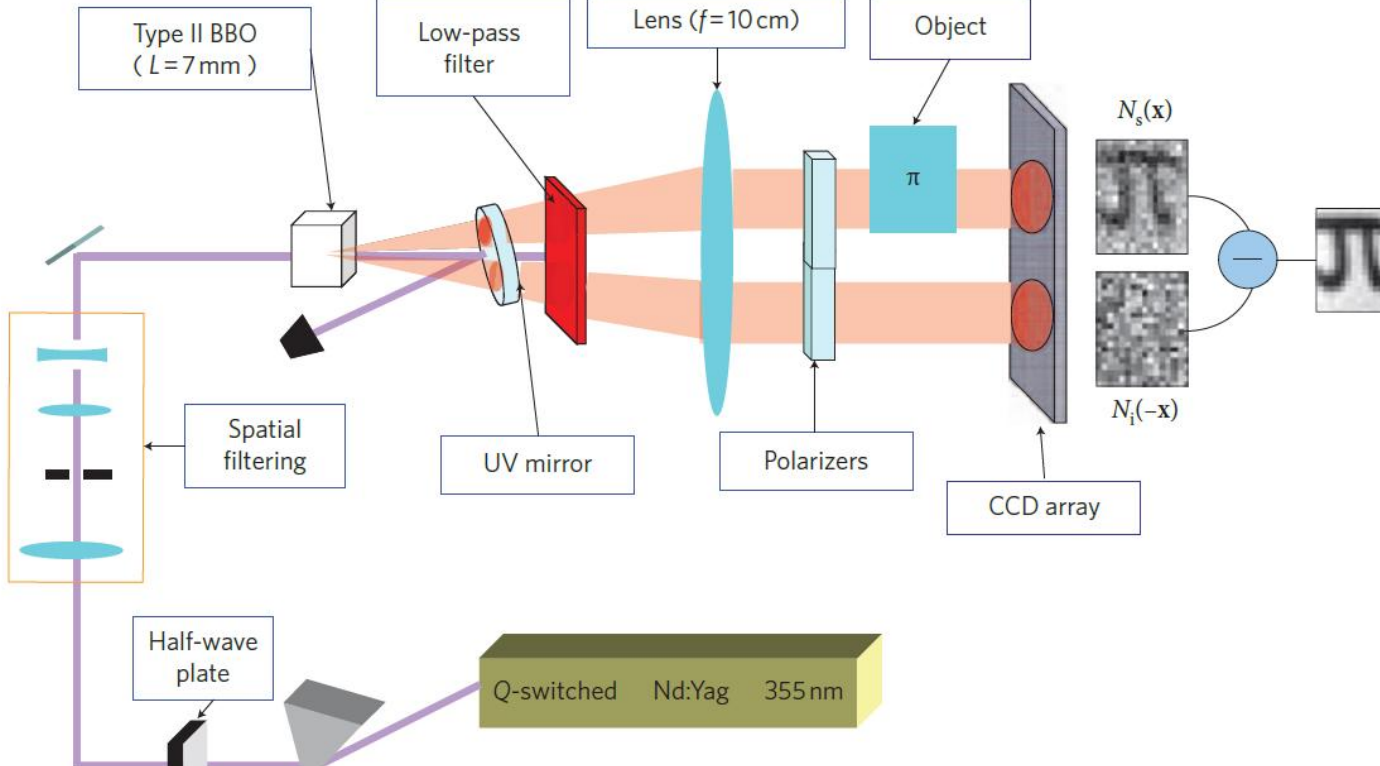
Experimental realization of sub-shot-noise

quantum imaging

G. Brida, M. Genovese and I. Ruo Berchera*



Ratio R between the signal-to-noise ratio in quantum imaging, and differential (dcl) and direct (cl) classical imaging. R is plotted as a function of the degree of correlation





Programmable Cluster State with Josephson Metamaterials - Superconducting Devices for Quantum Optics ECT* - Trento 8 October 2025 Amplifiers in the Quantum Regime – E. ENRICO

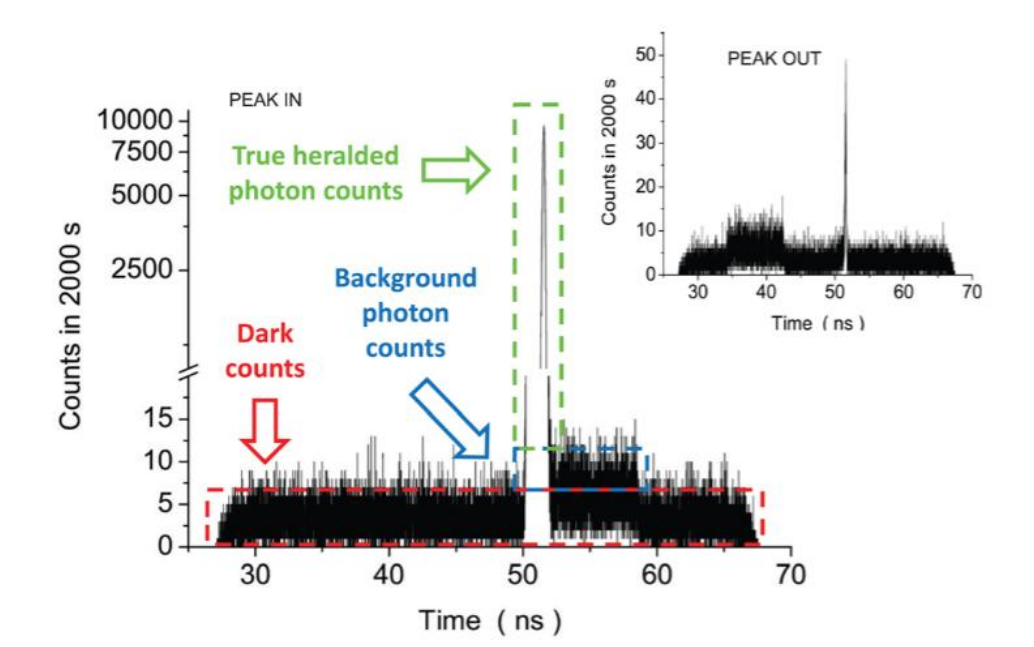
SPDC and Metrology – Counting

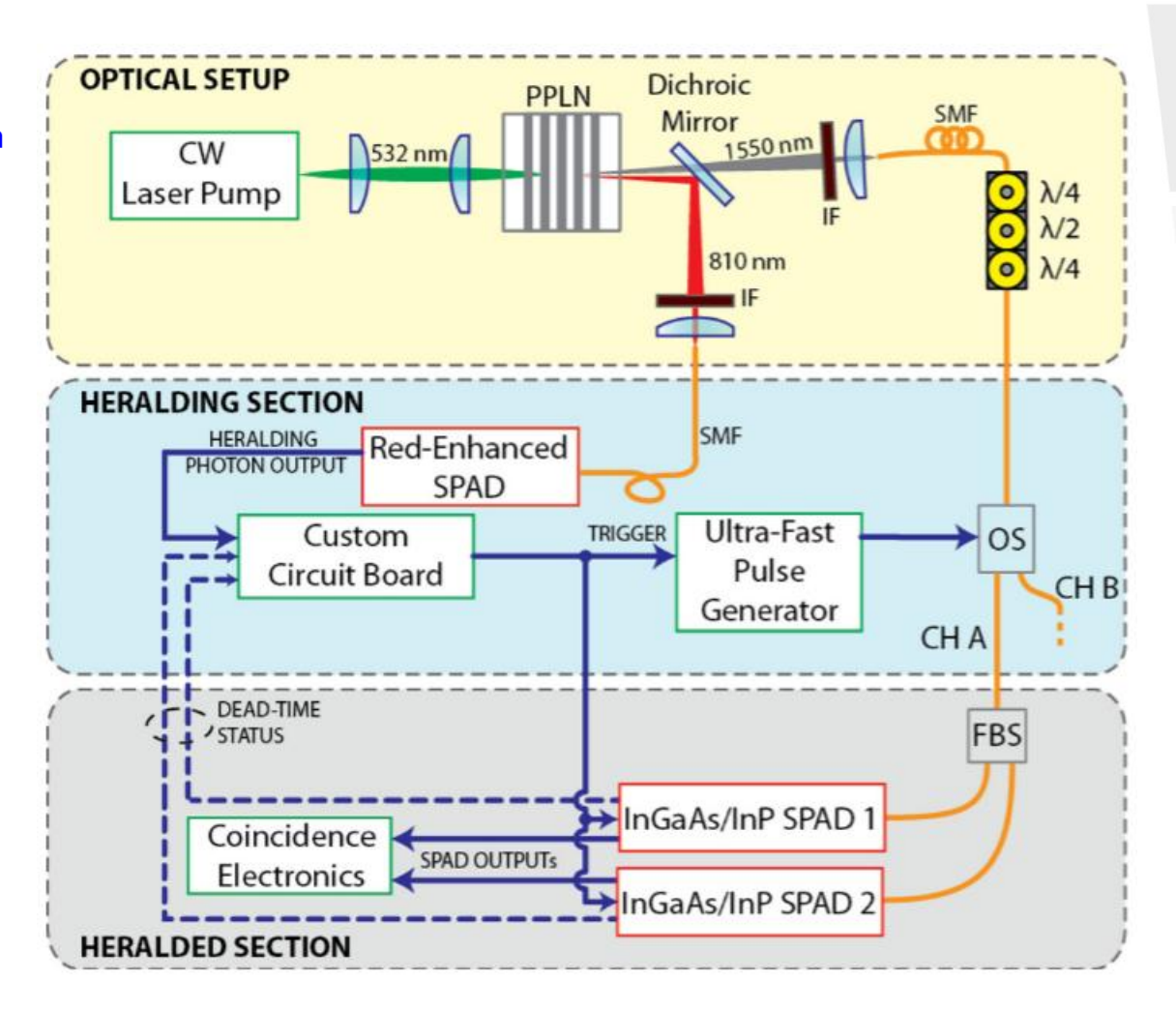
APPLIED PHYSICS LETTERS 101, 221112 (2012)

An extremely low-noise heralded single-photon source: A breakthrough for quantum technologies

G. Brida, ¹ I. P. Degiovanni, ¹ M. Genovese, ¹ F. Piacentini, ¹ P. Traina, ¹ A. Della Frera, ² A. Tosi, ² A. Bahgat Shehata, ² C. Scarcella, ² A. Gulinatti, ² M. Ghioni, ² S. V. Polyakov, ³ A. Migdall, ³ and A. Giudice ⁴

⁴Micro Photon Devices Srl, Via Stradivari 4, 39100 Bolzano, Italy



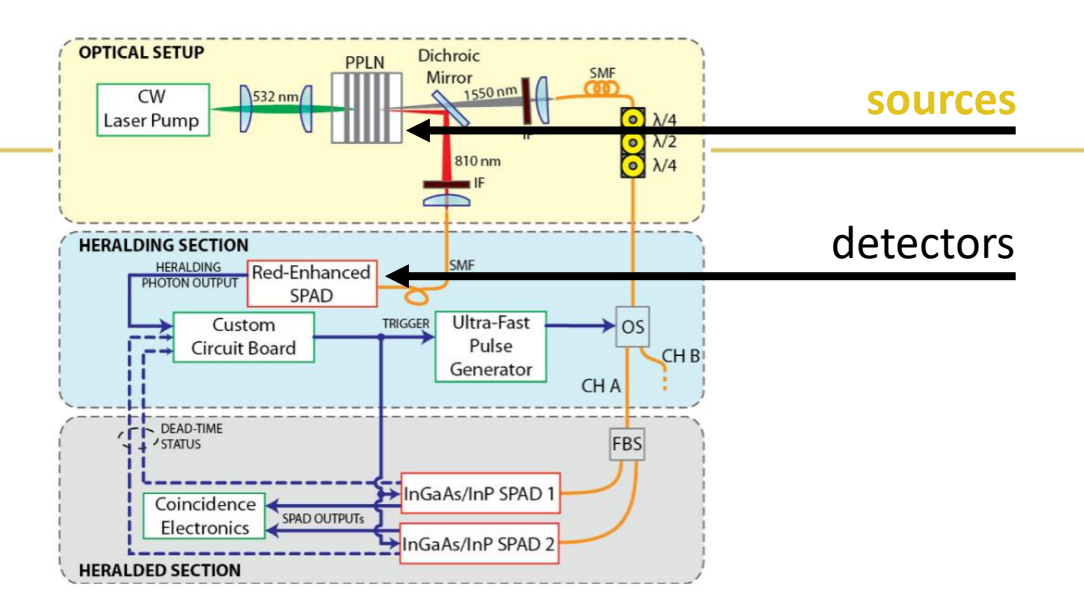




¹Istituto Nazionale di Ricerca Metrologica-I.N.RI.M., Strada delle Cacce 91, 10135 Torino, Italy

²Politecnico di Milano, Piazza Leonardo da Vinci 32, 20133 Milano, Italy

³Joint Quantum Institute, University of Maryland, and National Institute of Standards and Technology, 100 Bureau Dr, Stop 8410, Gaithersburg, Maryland 20899, USA



Superconducting Devices for Quantum Optics

(with a metrological flavor)



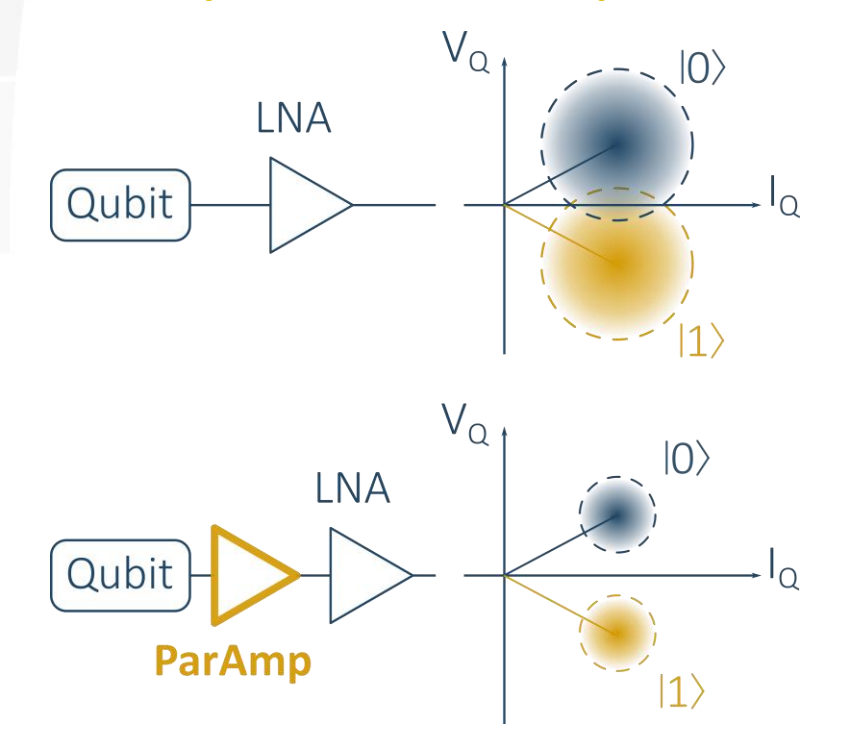
Josephson Nonlinear Metamaterials



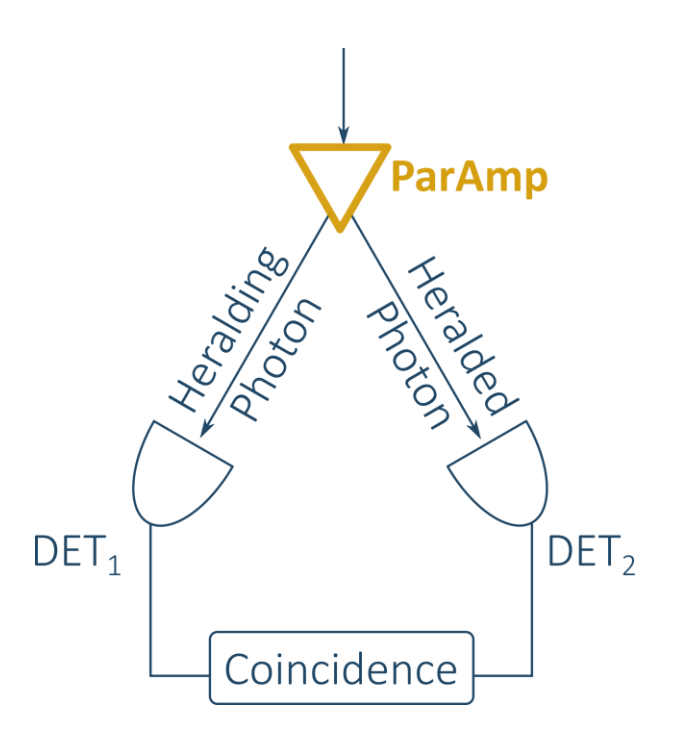


J-Metamaterials and Metrology

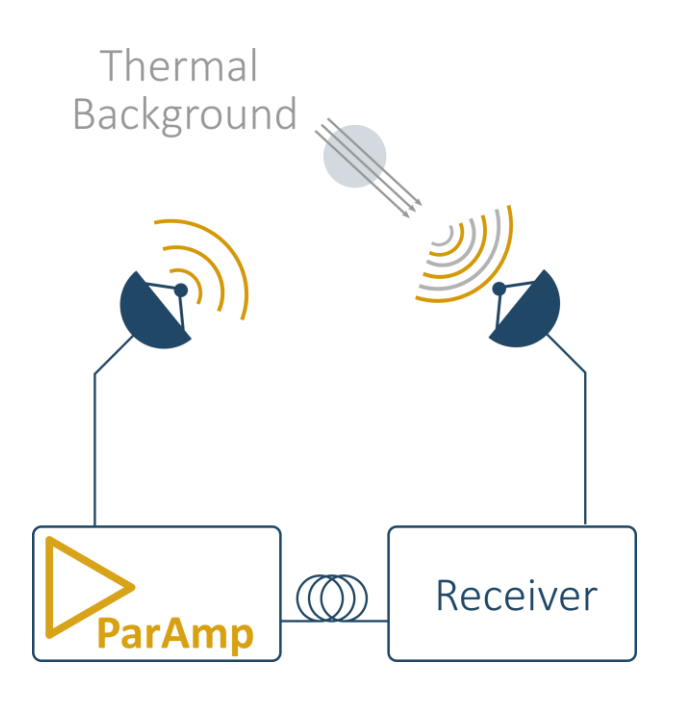
Improvement of readout of weak microwave signals with a quantum limited amplifier



Realization of absolute calibration technique of microwave number resolved photon detectors



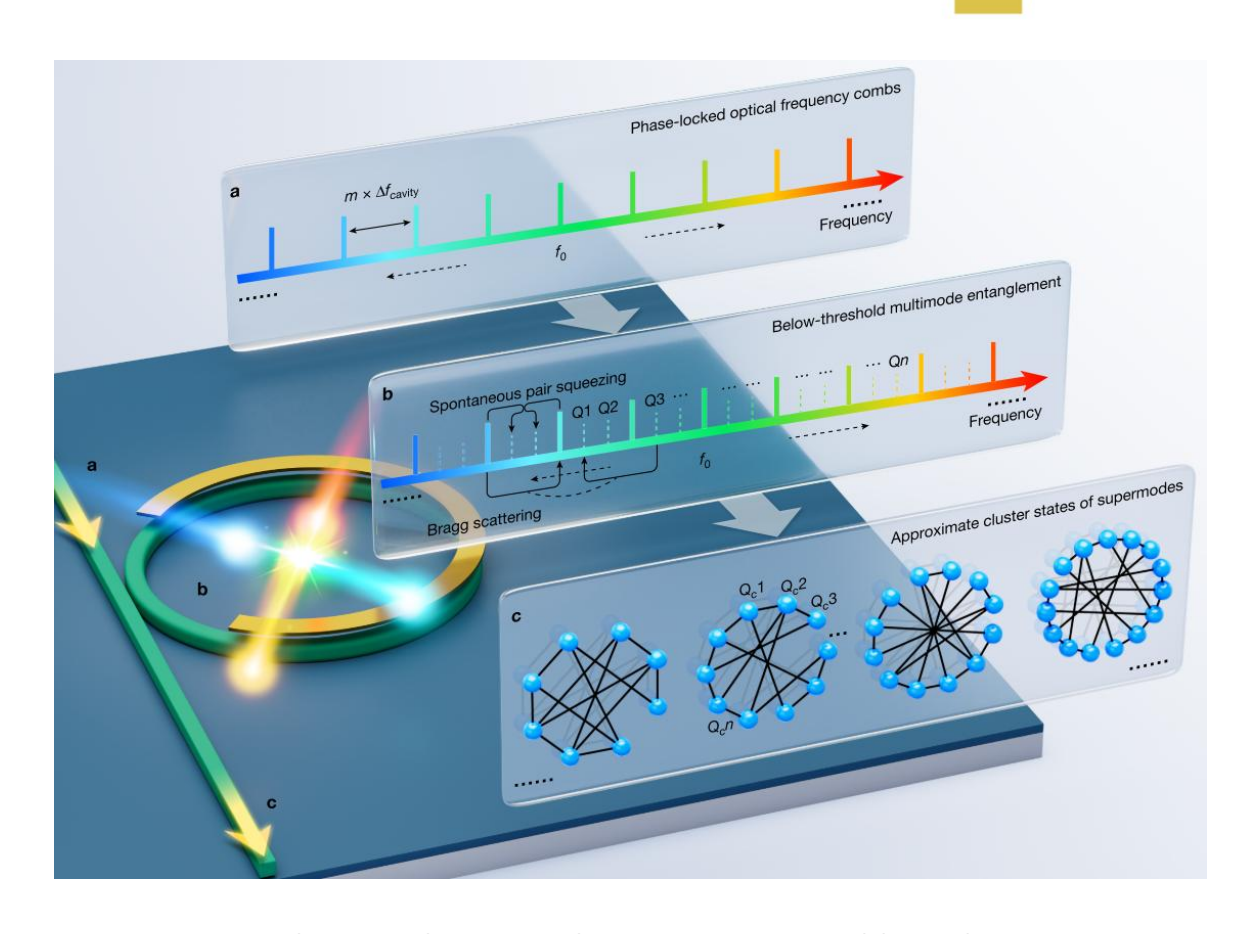
Microwave Quantum Illumination to improve detection or sensing in noisy environments





Cluster States - Overview

- Qubit Cluster States: Highly entangled states on discrete-variable systems (two-level qubits)
- CV Cluster States: Analogous entangled states in continuous-variable systems (e.g., squeezed light modes)
- Both serve as universal resources for measurement-based quantum computation (MBQC)
- Built via entangling operations on graph-like structures (e.g., controlled-Z for qubits, beam splitters + squeezing for CV)

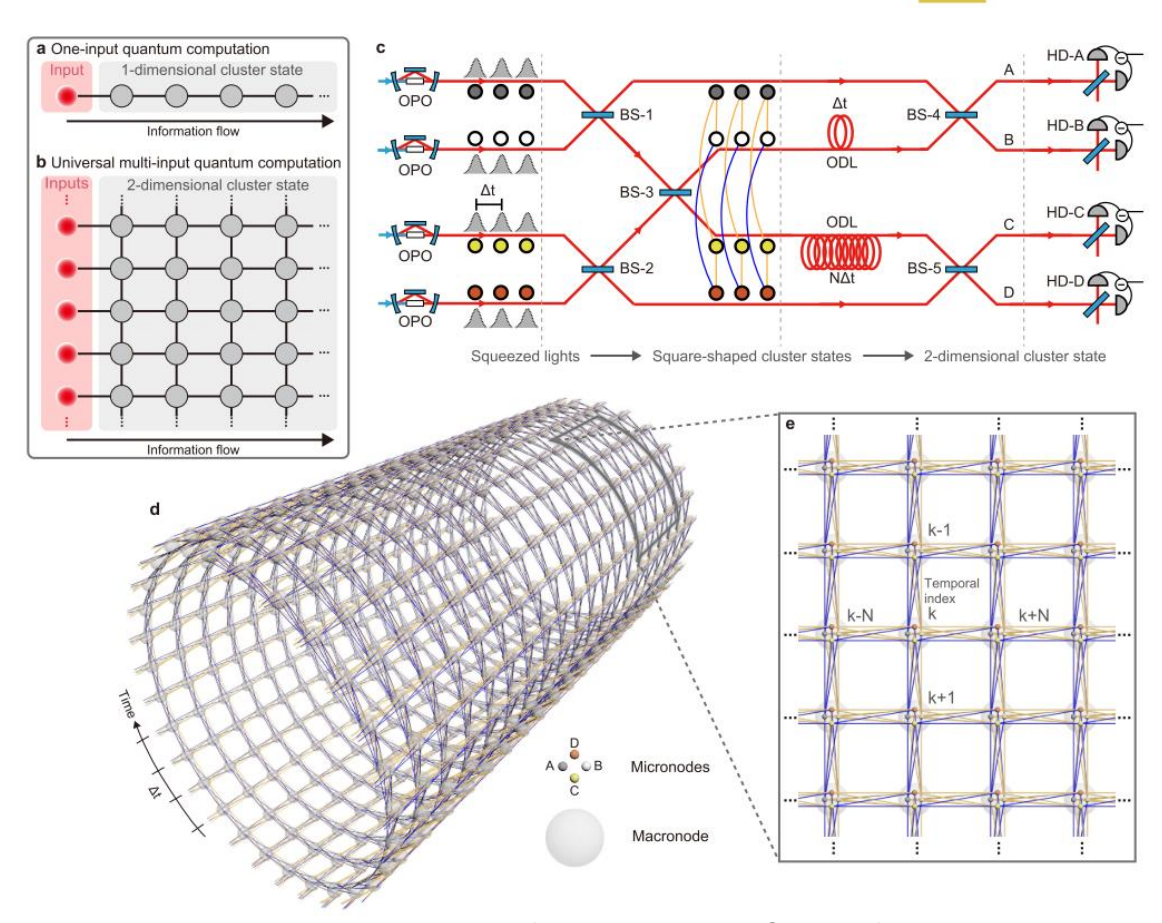


Jia, X., Zhai, C., Zhu, X. et al. Continuous-variable multipartite entanglement in an integrated microcomb. Nature 639, 329—336 (2025). https://doi.org/10.1038/s41586-025-08602-1



Cluster States - Applications

- MBQC: Perform quantum algorithms via local measurements on a pre-prepared entangled state
- Quantum Communication: Enable one-way quantum repeaters and teleportation networks (qubit & CV)
- Quantum Simulation: Emulate complex many-body systems and quantum dynamics
- Quantum Error Correction: Foundation for topological codes (qubit) and bosonic codes (CV)
- Quantum Sensing & Metrology: Exploit multipartite entanglement for enhanced sensitivity (especially in CV systems)

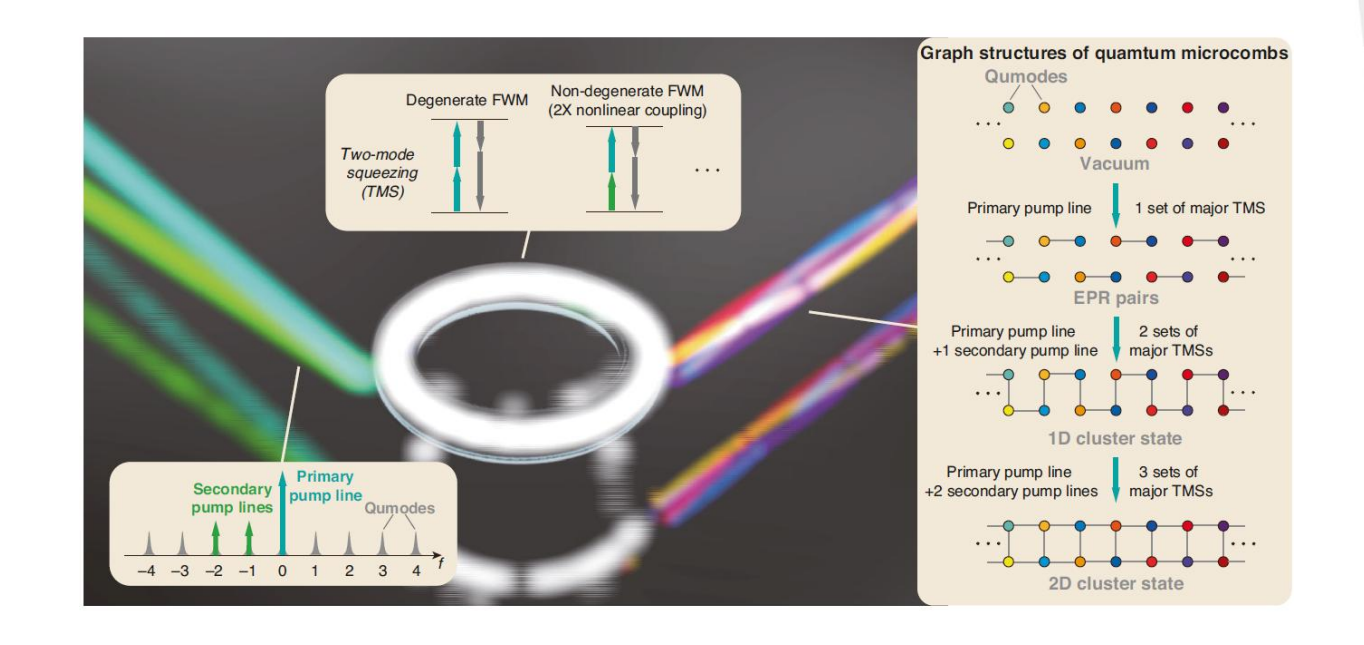


Warit Asavanant et al., Generation of time-domain-multiplexed two-dimensional cluster state. Science 366,373-376 (2019). DOI:10.1126/science.aay2645



Cluster States – Advantages

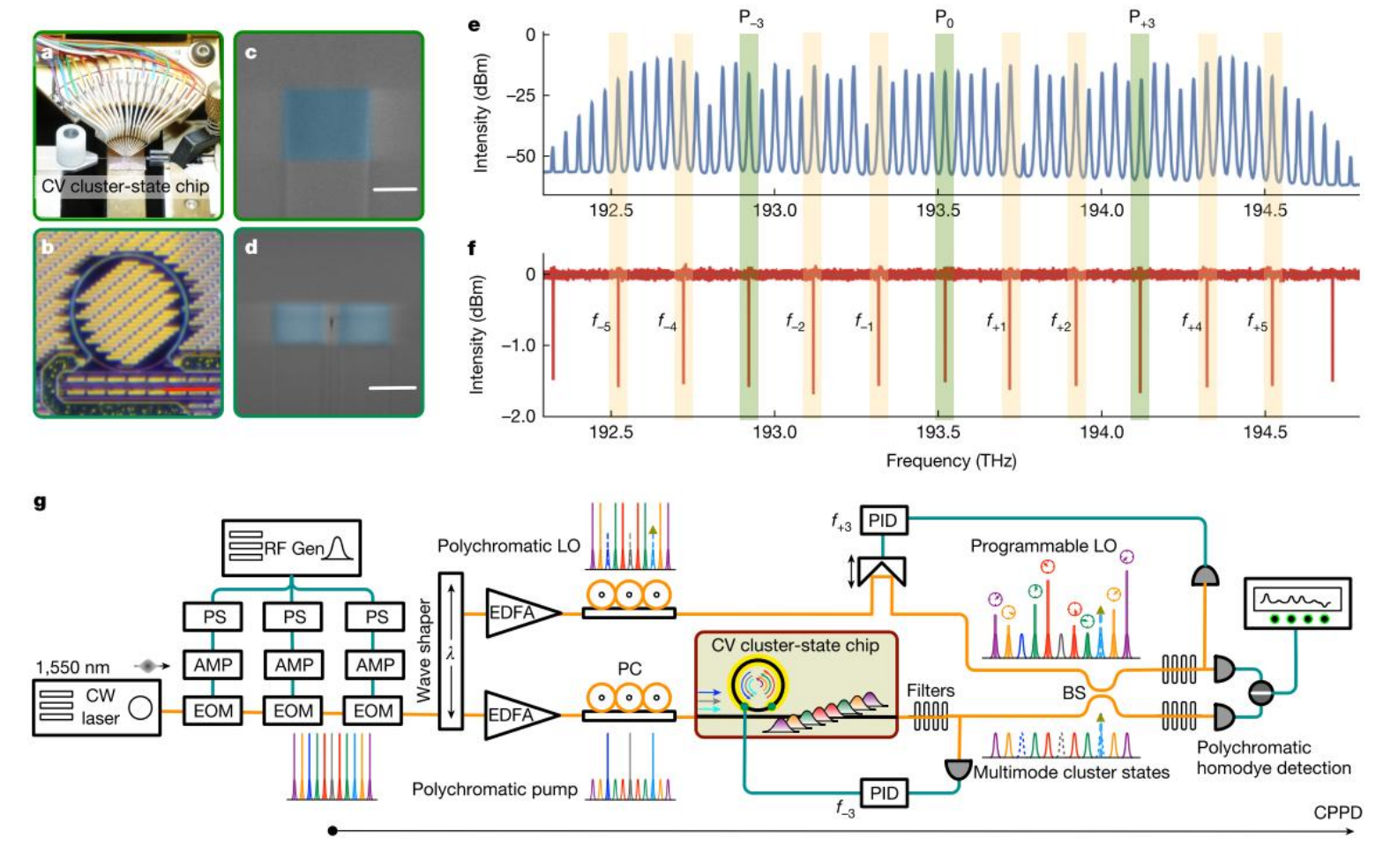
- Decoupled Architecture: Prepare entanglement once, compute via measurements → simplifies control
- Parallelism: Many measurements can be performed simultaneously in spatial or temporal structures
- Scalability: CV cluster states can be generated in large scale (e.g., using optical frequency combs or time-domain multiplexing)
- Hardware Efficiency: Measurement-based protocols reduce gate complexity and hardware overhead
- Noise Robustness: Topological and faulttolerant constructions possible for both qubit and CV implementations



Wang, Z., Li, K., Wang, Y. et al. Large-scale cluster quantum microcombs. Light Sci Appl 14, 164 (2025). https://doi.org/10.1038/s41377-025-01812-2



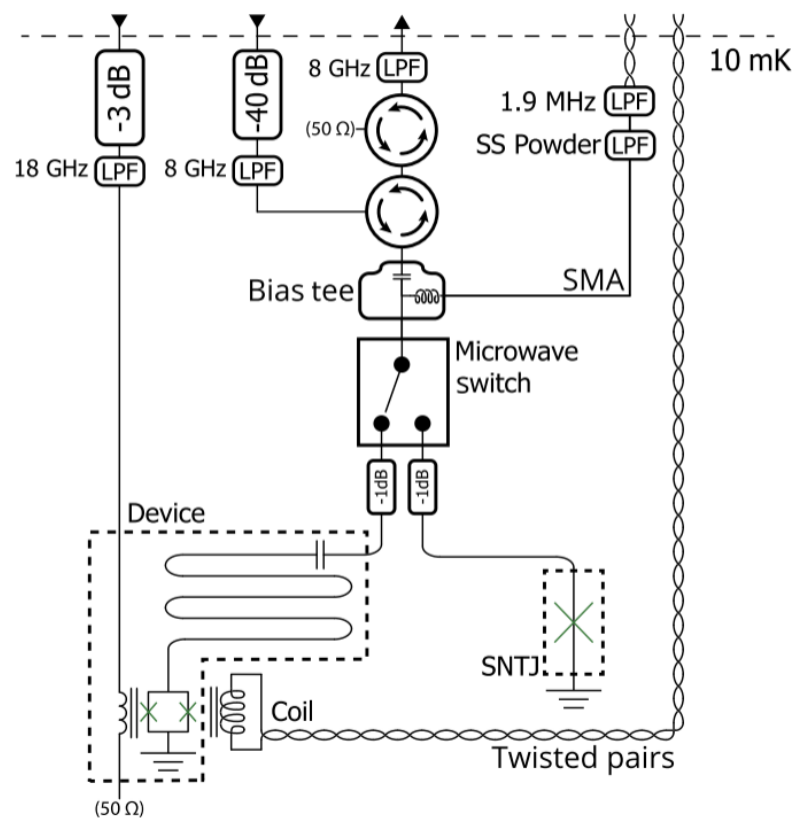
Cluster States – Optics Regime



Jia, X., Zhai, C., Zhu, X. et al. Continuous-variable multipartite entanglement in an integrated microcomb. Nature 639, 329–336 (2025). https://doi.org/10.1038/s41586-025-08602-1



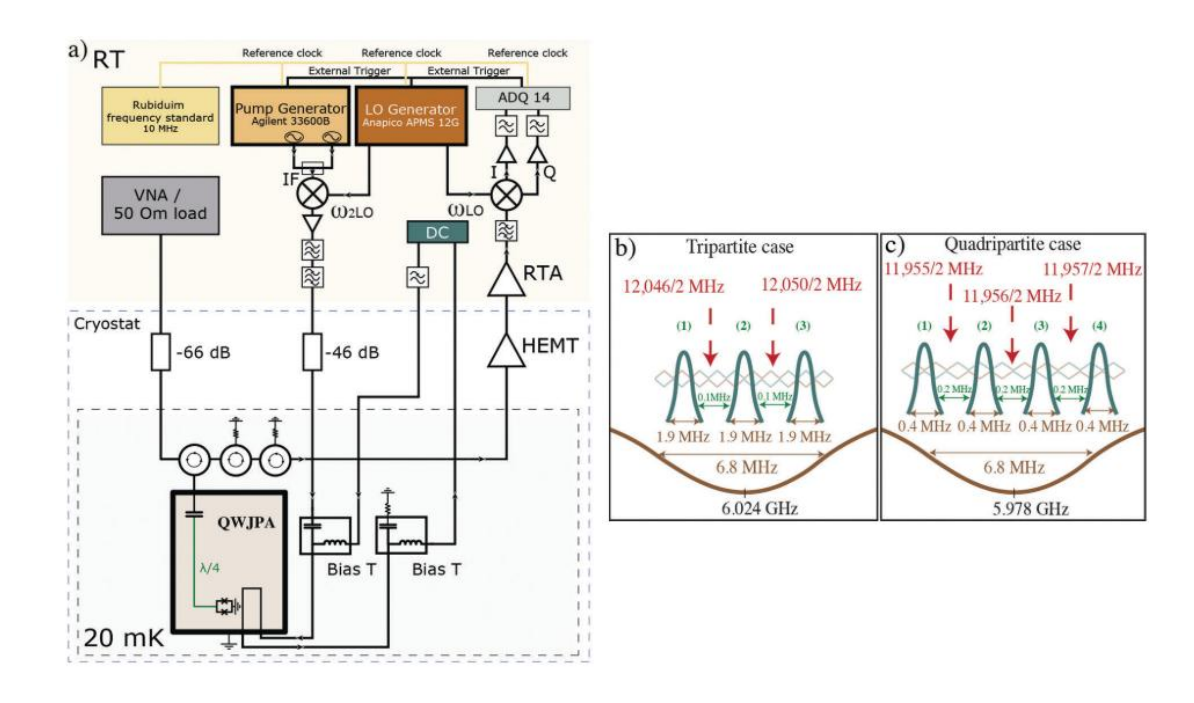
Cluster States – Microwave Regime



Sandbo Chang, C. W., Simoen, M., Aumentado, J., et.al. (2018).

Generating Multimode Entangled Microwaves with a Superconducting
Parametric Cavity. Physical Review Applied, 10(4).

https://doi.org/10.1103/PhysRevApplied.10.044019



Petrovnin, K. V., Perelshtein, M. R., Korkalainen, T., Vesterinen, V., Lilja, I., Paraoanu, G. S., & Hakonen, P. J. (2023). Generation and Structuring of Multipartite Entanglement in a Josephson Parametric System. Advanced Quantum Technologies, 6(1). https://doi.org/10.1002/qute.202200031



Programmable Microwave CS

- (a) Multiple pump tones from an AWG drive the JTWPA[1] into a three-wave mixing regime, generating CV cluster states in the frequency domain.
- (b) Experimental setup: broadband mode synthesis, cryogenic routing, and multiplexed heterodyne detection with noise rejection via reference state protocol.

[1] VTT /Arctic TWPA from

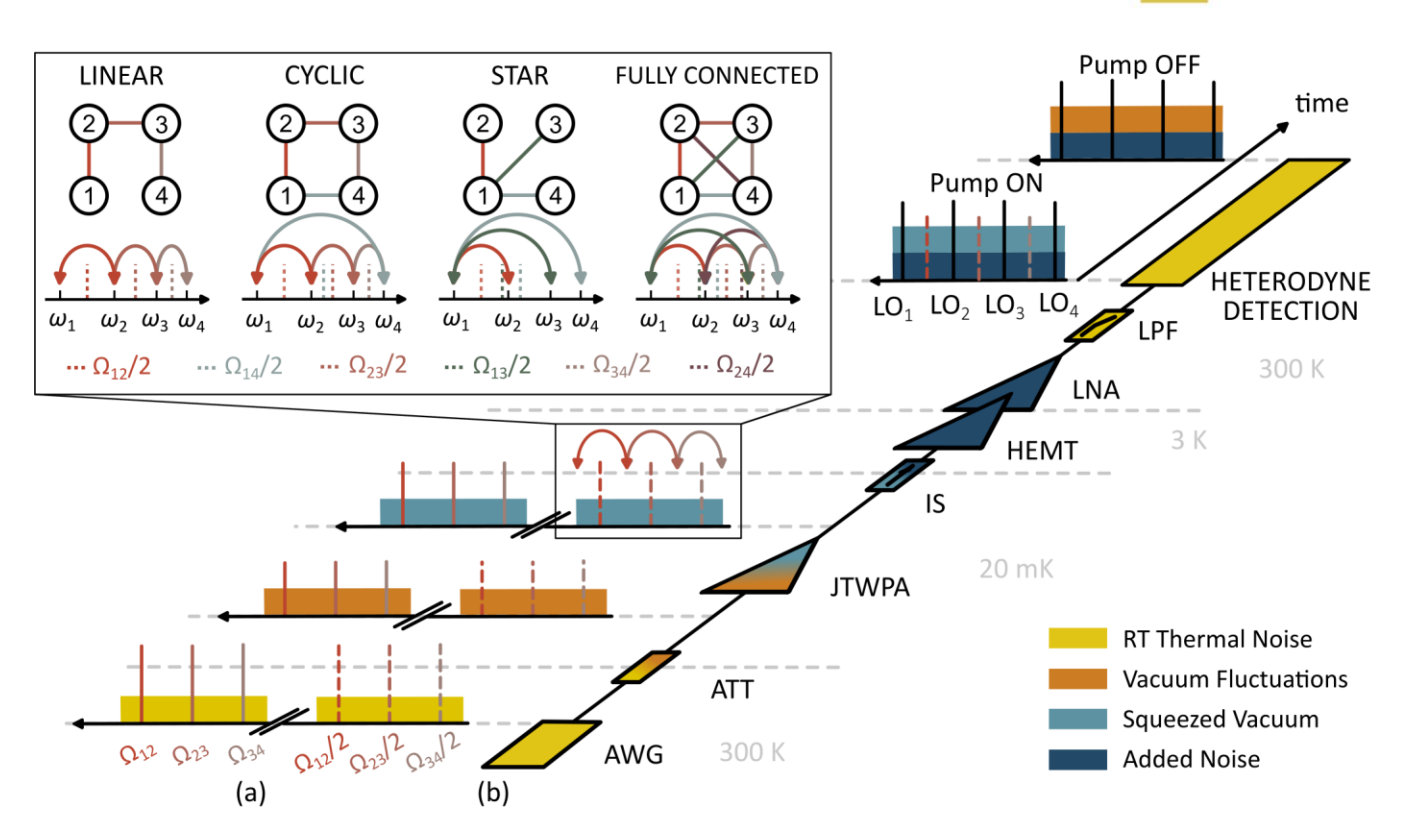


EUROPEAN PARTNERSHIP







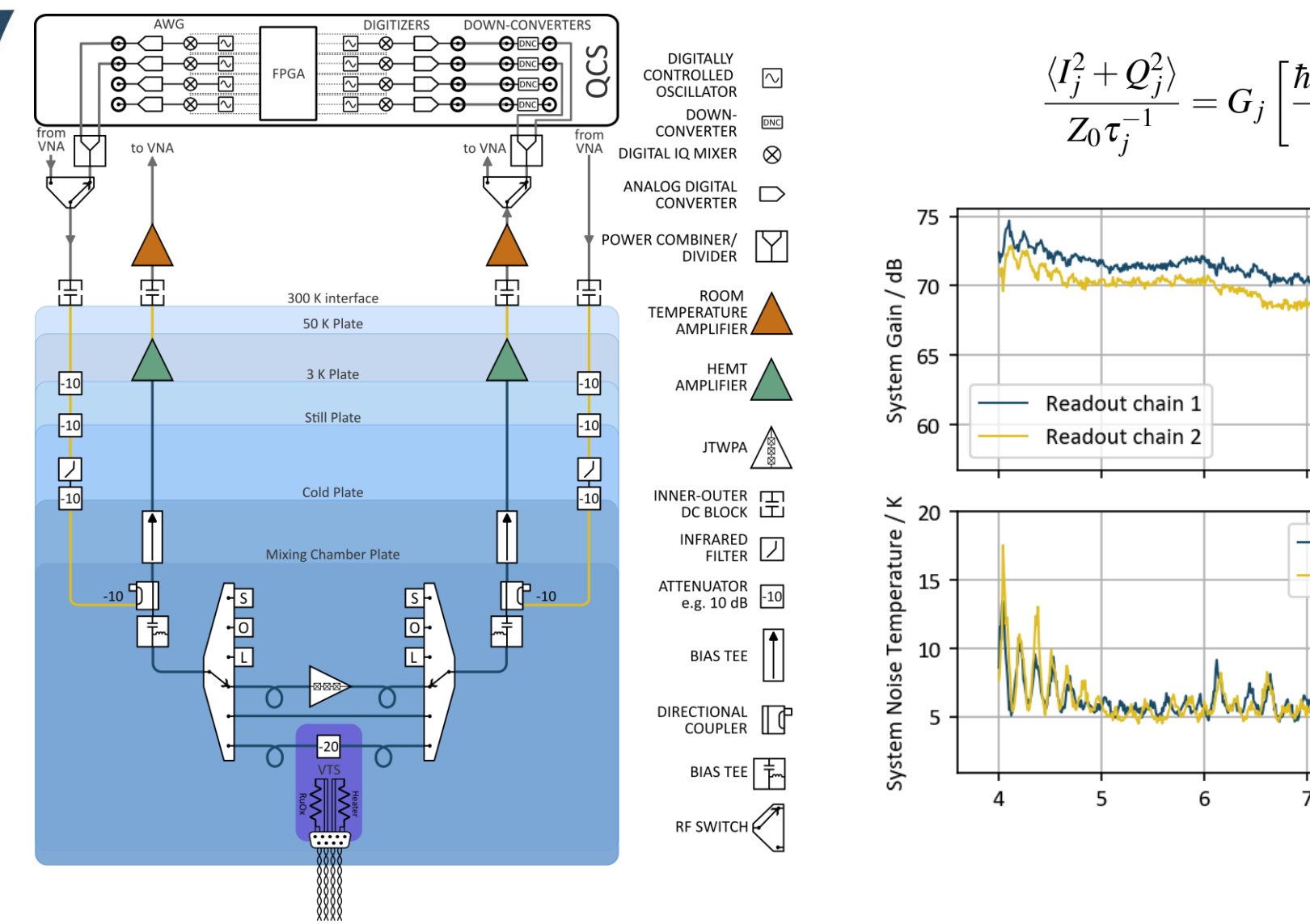


$$\hat{H}_{ ext{eff}} = \sum_{k=1}^n \sum_{j \leq l} \left(r_{jl}^{(k)} \hat{a}_j^\dagger \hat{a}_l^\dagger + r_{jl}^{(k)*} \hat{a}_j \hat{a}_l
ight)$$

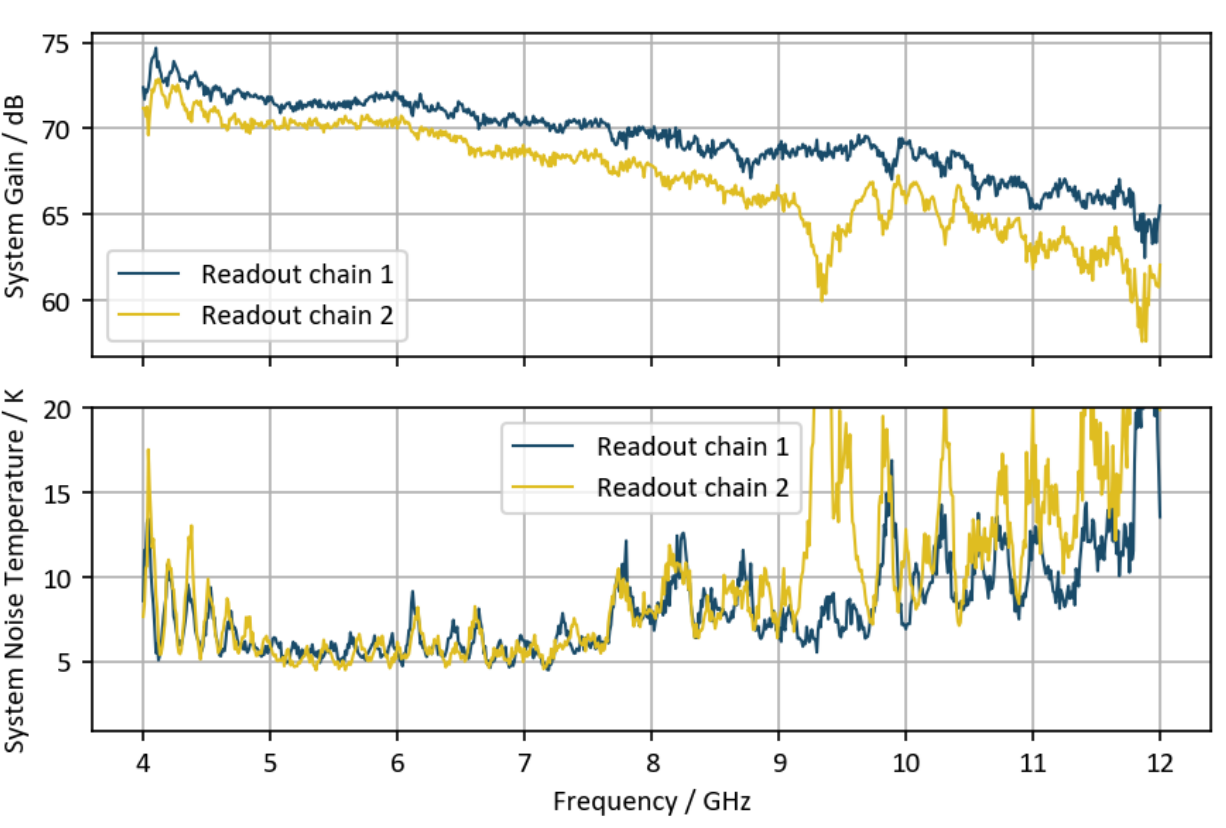
$$r_{il}^{(k)} = g_{il}^{(k)} \alpha_k e^{-i\phi_k}$$



Cryogenic setup and Plank spectroscopy



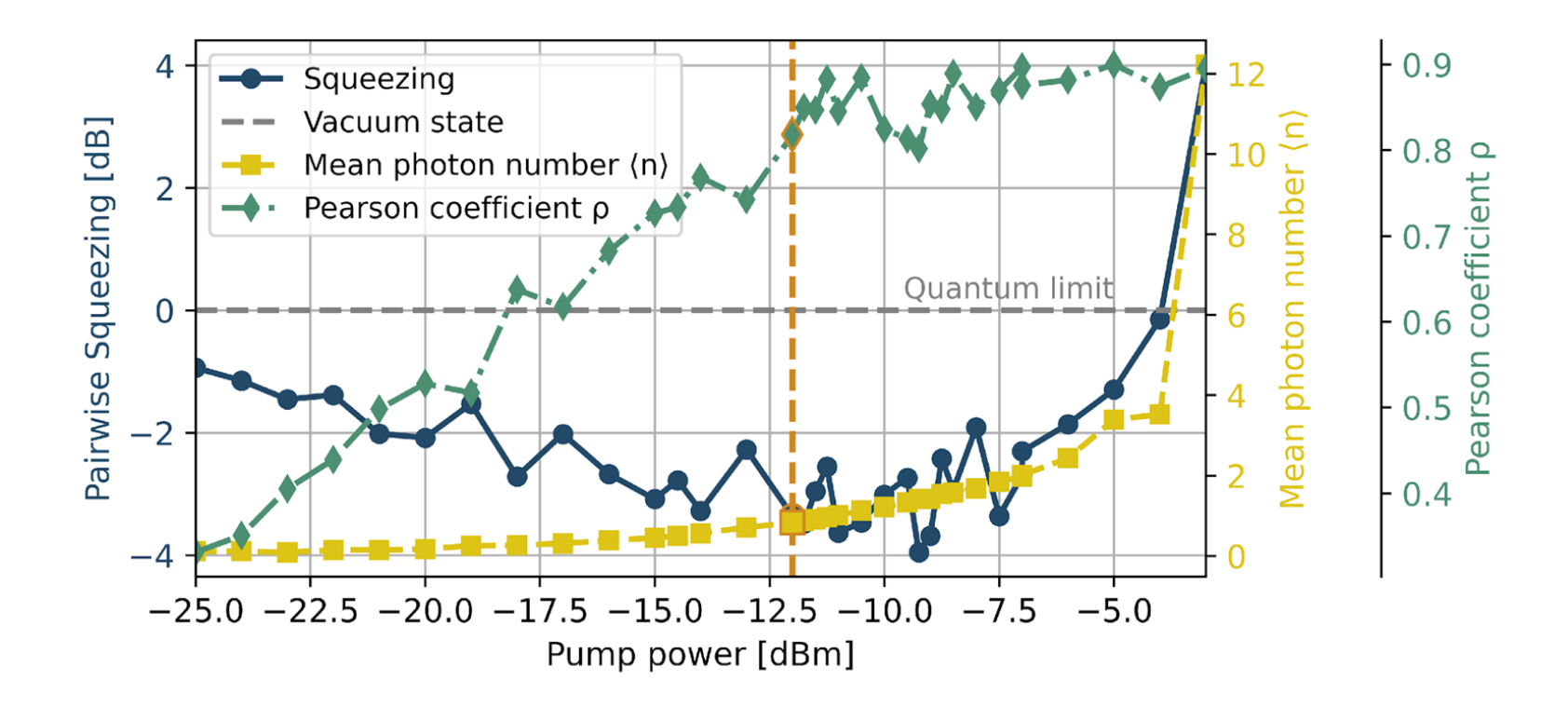
$$\frac{\langle I_j^2 + Q_j^2 \rangle}{Z_0 \tau_j^{-1}} = G_j \left[\frac{\hbar \omega_j}{2} \coth \left(\frac{\hbar \omega_j}{2k_{\rm B} T_{\rm VTS}} \right) + k_{\rm B} T_{\rm SYS,j} \right]$$





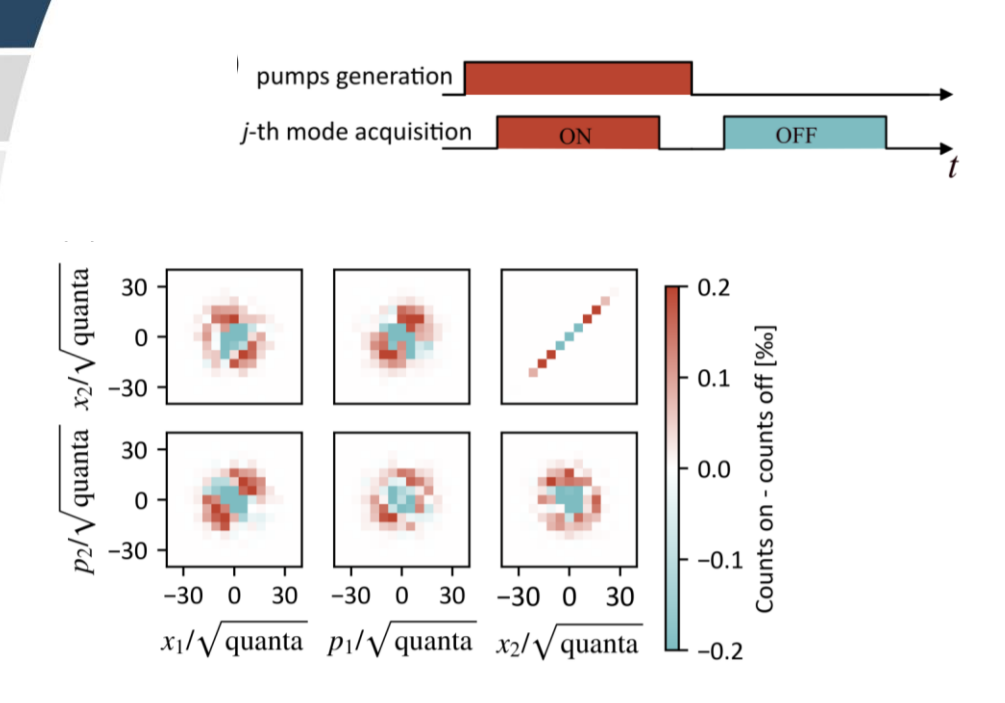
Programmable Cluster State with Josephson Metamaterials - Superconducting Devices for Quantum Optics ECT* - Trento 8 October 2025 Amplifiers in the Quantum Regime – E. ENRICO

Single pump setup validation

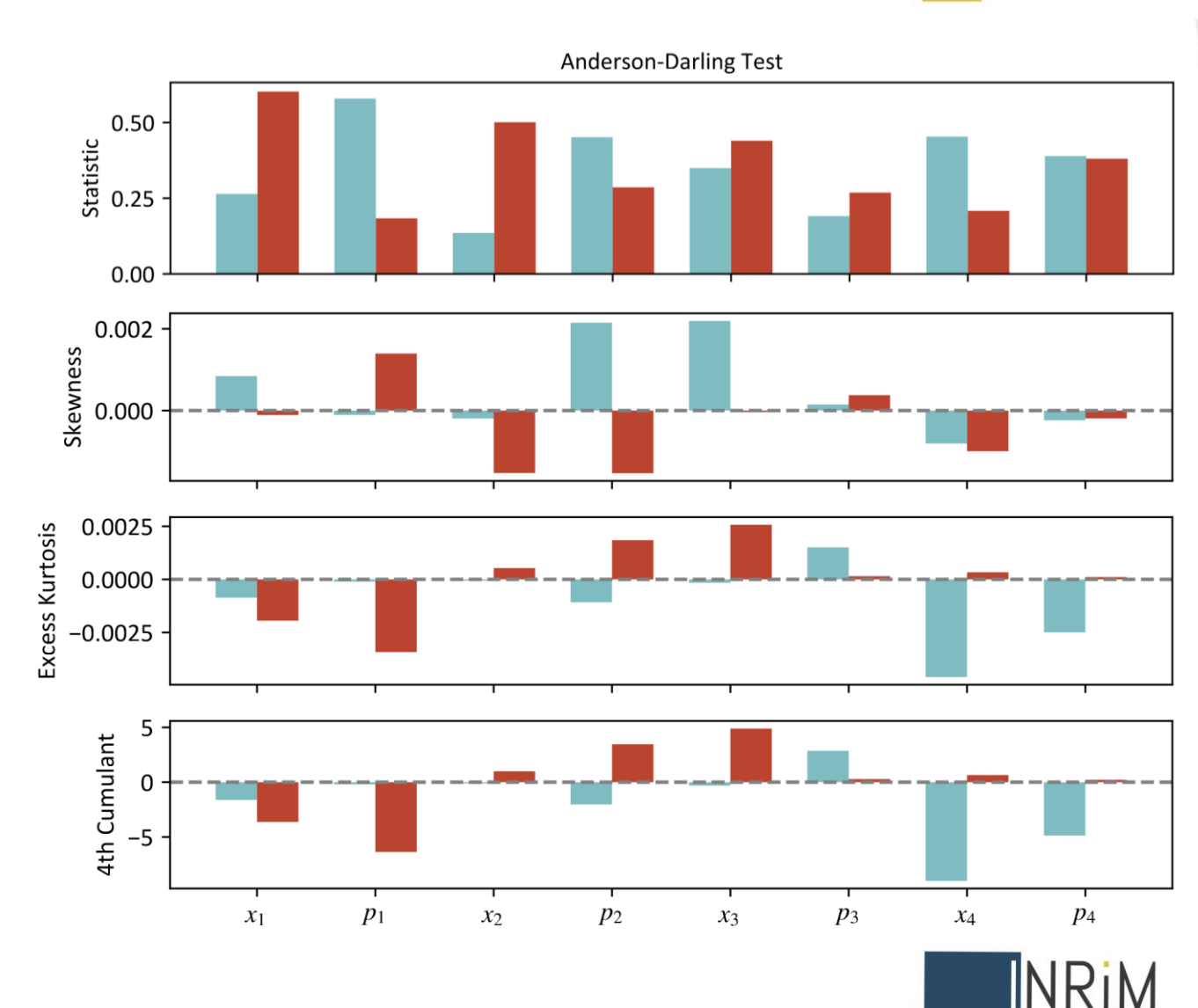




Gaussianity Validation

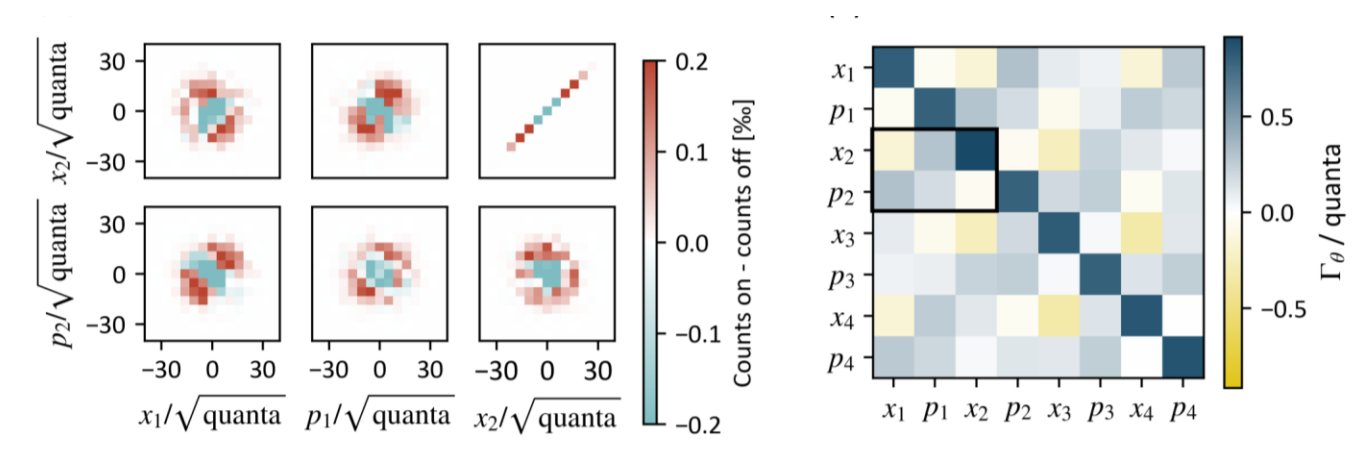


- Standard normality tests, namely the Shapiro–Wilk and Anderson–Darling tests.
- Moment analysis up to fourth order, including skewness, excess kurtosis, and fourth-order cumulants.



Covariance Matrix Reconstruction





$$i_j = \frac{I_j}{\sqrt{2G_jZ_0\hbar\omega_j/2\tau^{-1}}}, \quad q_j = \frac{Q_j}{\sqrt{2G_jZ_0\hbar\omega_j\tau^{-1}}}$$

$$\Gamma_{j,l}^{\mathrm{exp}} = rac{1}{2} \left\langle M_j M_l + M_l M_j \right\rangle - \left\langle M_j \right\rangle \left\langle M_l \right\rangle$$

$$\mathbf{M} = (i_1, q_1, \dots, i_m, q_m)^T$$

Measure output quadratures with pump OFF

→ reference vacuum state.

Measure with pump ON

→ signal (CS) + TWPA-added noise.

Comparing the two

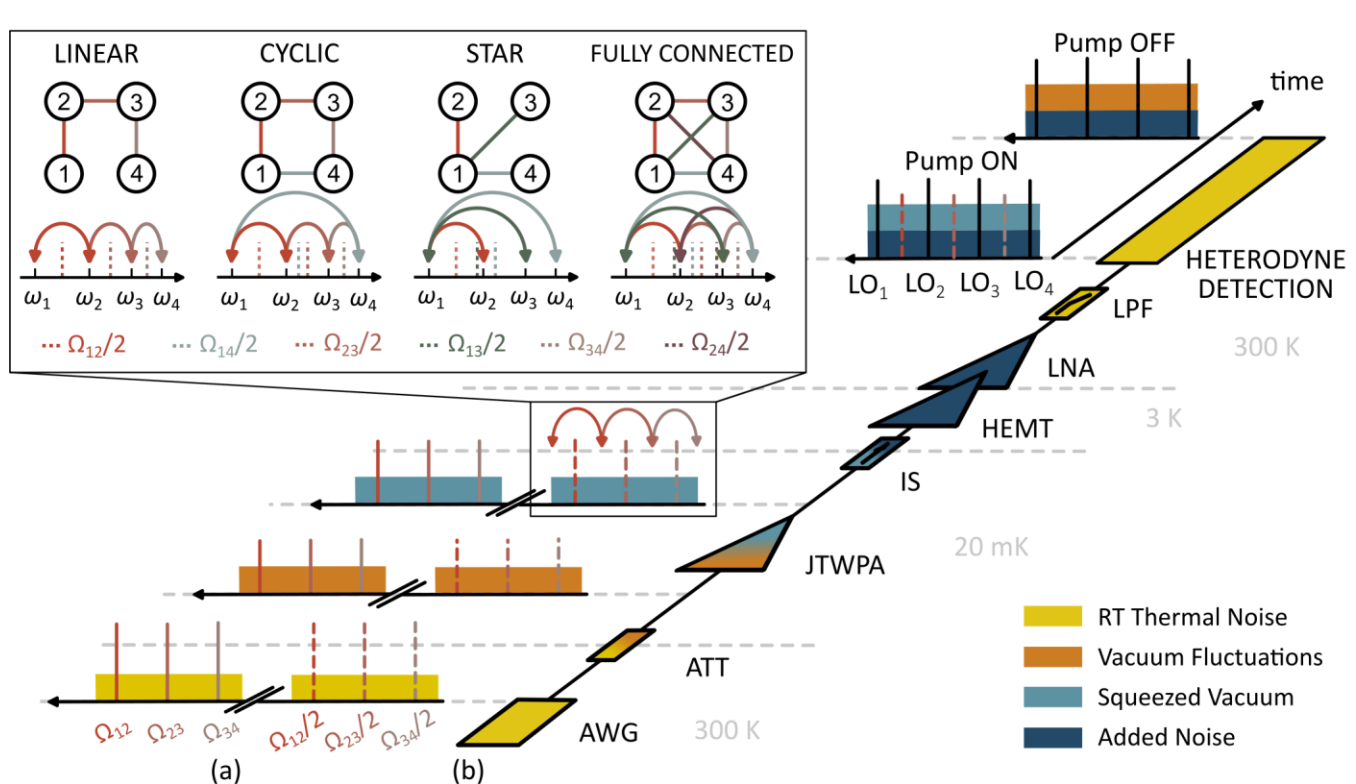
→ reconstruction of the output covariance matrix, isolating the TWPA's effect (amplification, squeezing, added noise).

$$\Gamma_{ heta} = (\Gamma_{ ext{ON}}^{ ext{exp}} - \Gamma_{ ext{OFF}}^{ ext{exp}}) + \sigma^{ ext{in}}$$



Het. Det. with Unknown Phase Offsets

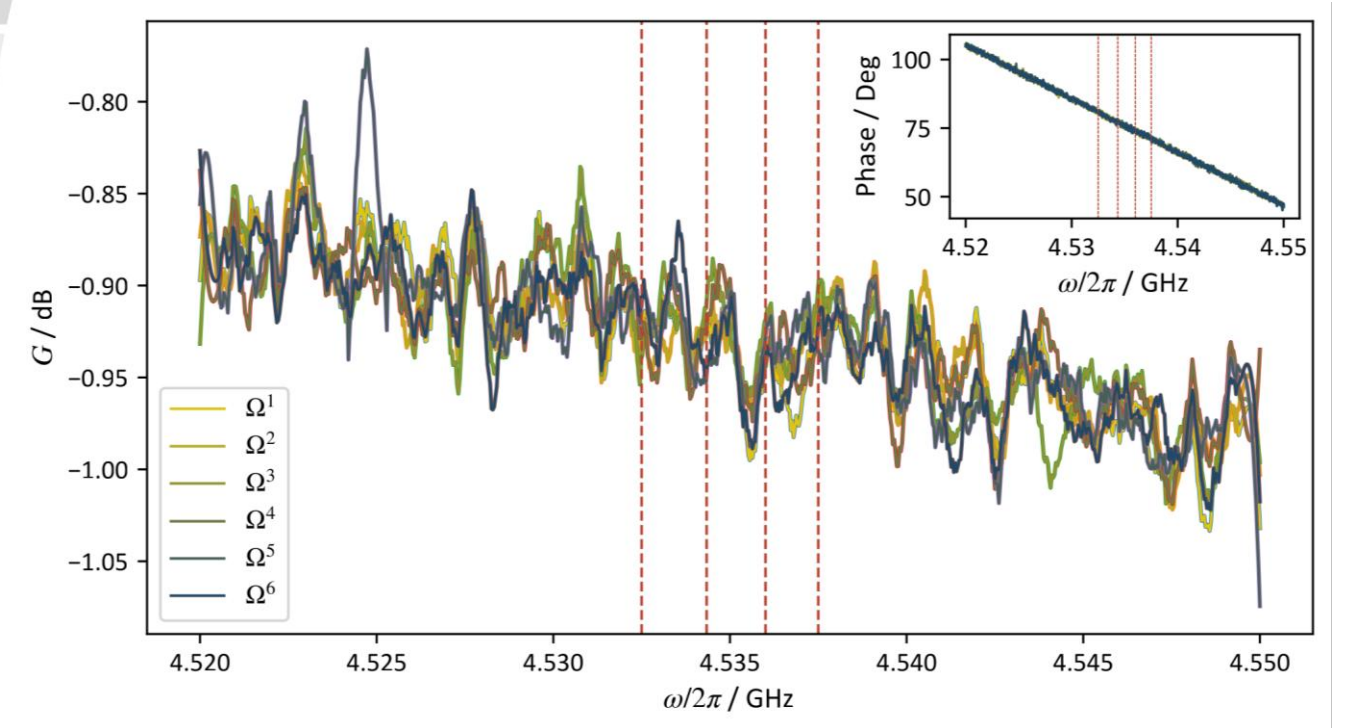
- LOs are phase-locked to the JTWPA pumps.
- Unknown phase shifts arise from setup components, cable dispersion, and group delays.
- These cause effective quadrature rotation across frequency.
- Covariance matrix affected.



$$\Gamma_{\theta} = \mathbf{R}_{\theta} \cdot \mathbf{\Gamma} \cdot \mathbf{R}_{\theta}^{\mathrm{T}}, \qquad \mathbf{R}_{\theta} = \bigoplus_{j=1}^{m} \begin{pmatrix} \cos \theta_{j} & -\sin \theta_{j} \\ \sin \theta_{j} & \cos \theta_{j} \end{pmatrix}$$



Assumptions & Squeezing Optimization



- Covariance matrix optimized via local phasespace rotations $R_i(\theta_i)$.
- Pumps phase-locked, frequencies close
 ⇒ stable relative phase drift.
- Symmetric (almost flat) squeezing
 ⇒ no need for local squeezing or shear.
- Restriction to orthogonal symplectic transforms preserves entanglement structure.
- → Goal: reorient squeezing axes to maximize observed two-mode correlations.



- Optimization aims to maximize $p_i x_l$ correlations over the set of LO phases θ .
- Define the average covariance function:

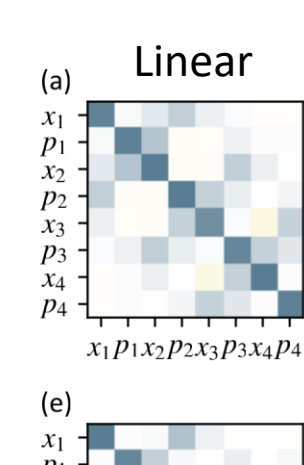
$$\mathscr{C}_{px}(\theta) = \frac{1}{m^2} \sum_{i=1}^{m} \sum_{l=1}^{m} \mathbf{\Gamma}_{\theta, p_j, x_l}$$

The optimal phase set θ_{opt} maximizes this correlation measure.

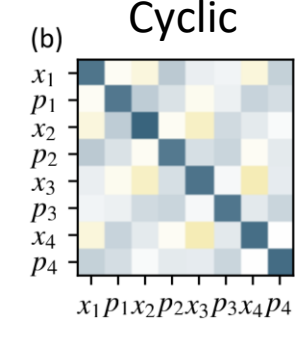
$$\theta_{\text{opt}} = \arg\max_{\theta} \mathscr{C}_{px}(\theta)$$

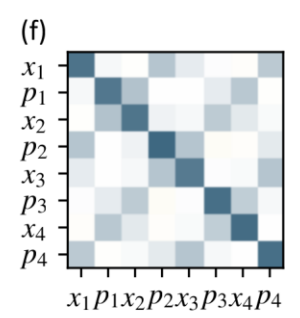
This identifies the global quadrature basis where the reconstructed covariance matrix Γ_{A} best matches an ideal cluster state.

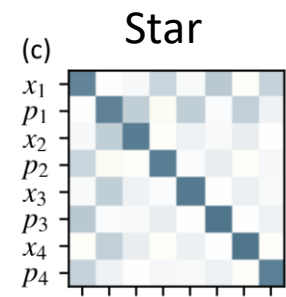
$$oldsymbol{\Gamma} = \mathbf{R}_{oldsymbol{ heta}_{ ext{opt}}}^{-1} oldsymbol{\Gamma}_{oldsymbol{ heta}_{ ext{opt}}} \left(\mathbf{R}_{oldsymbol{ heta}_{ ext{opt}}}^{-1}
ight)^{ op}$$



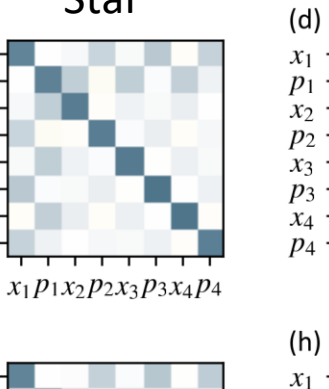
 $x_1p_1x_2p_2x_3p_3x_4p_4$

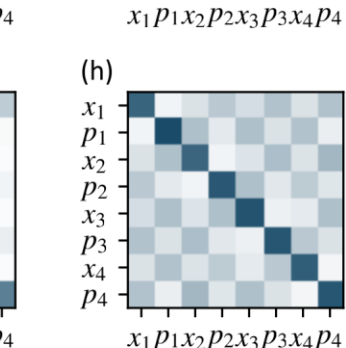


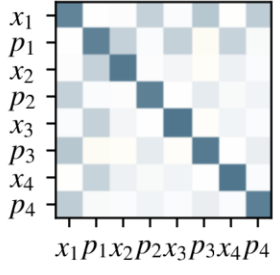




PRE









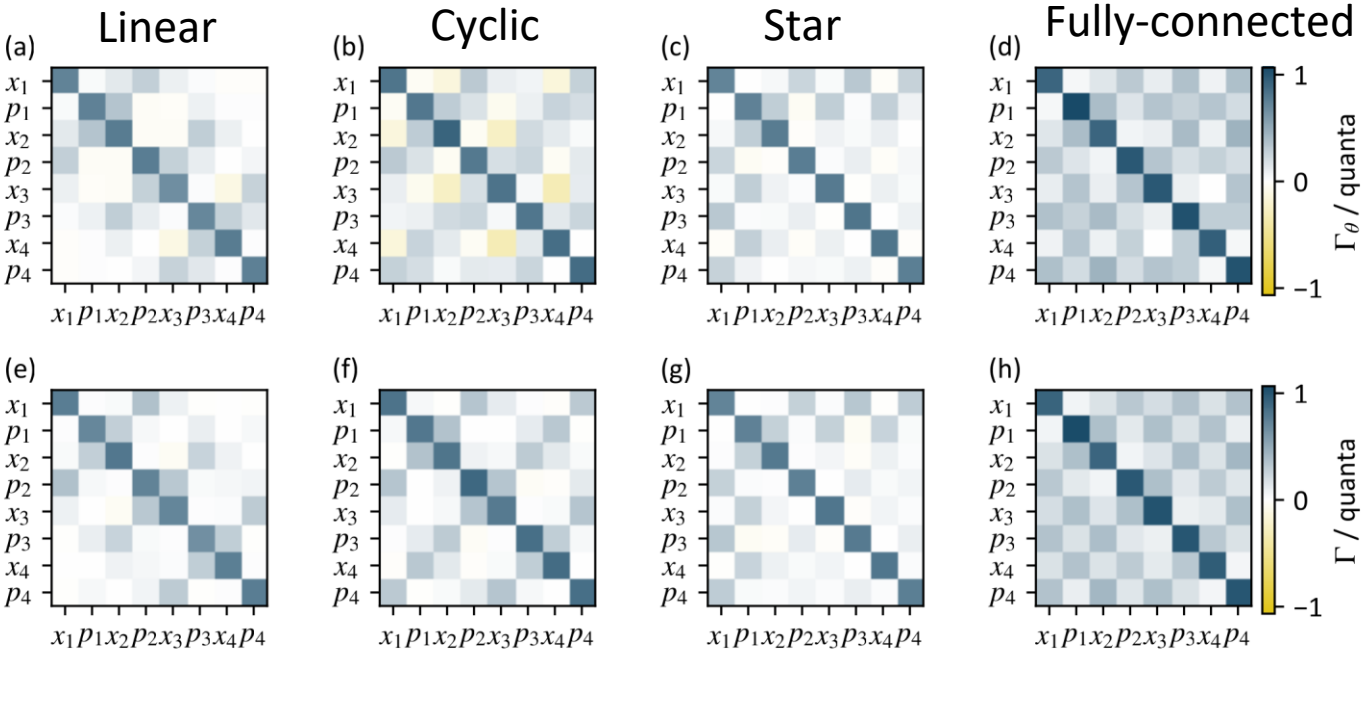
POST



Fully-connected

- Captures and compensates unknown pump-induced phase shifts
- Ensures physically consistent phase alignment across modes—key for coherent protocols (e.g. cluster states, error correction)

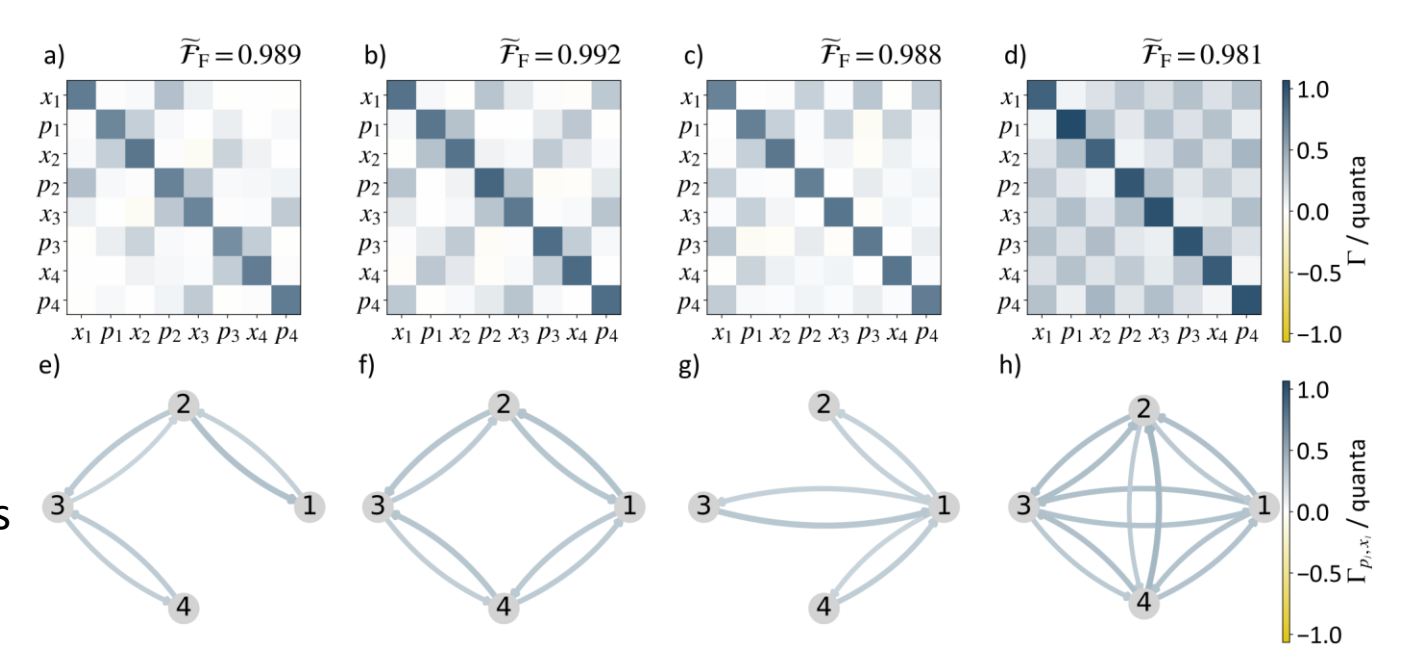




POST



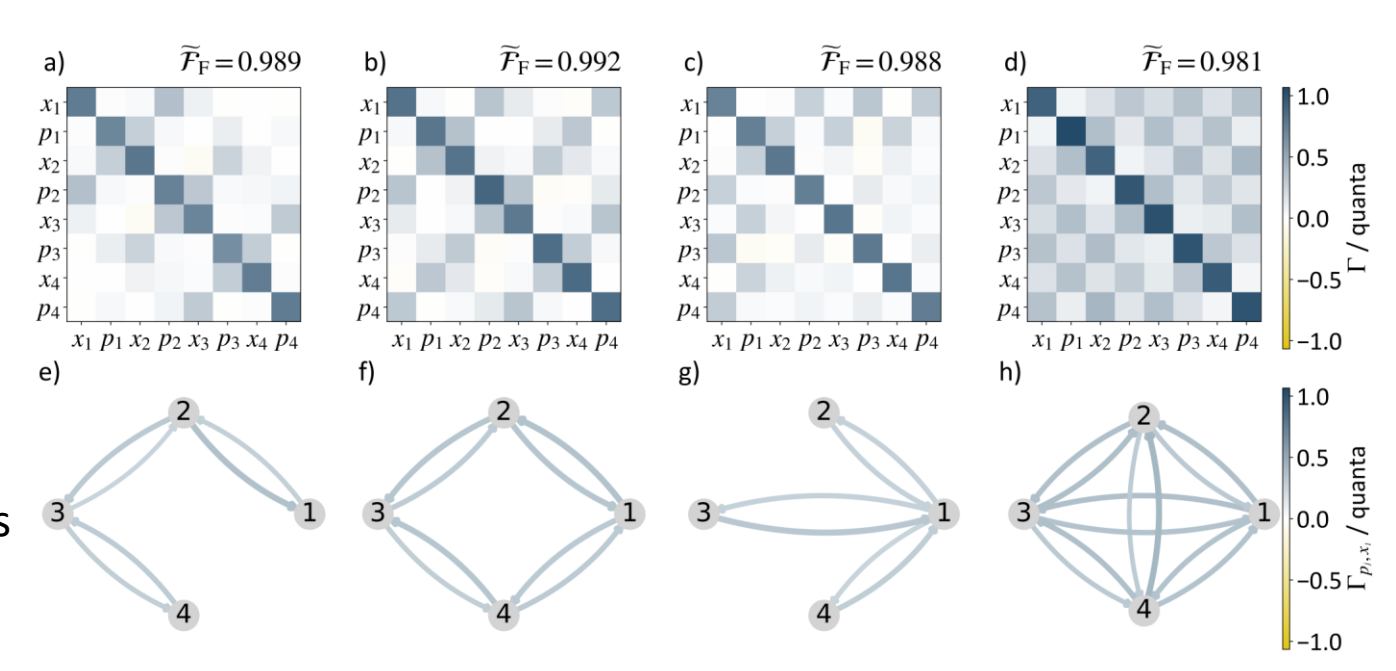
- Captures and compensates unknown pump-induced phase shifts
- Ensures physically consistent phase alignment across modes—key for coherent protocols (e.g. cluster states, error correction)
- The optimal global quadrature basis reveals maximal two-mode squeezing and graph structure





Is there a trivial way to compare with the theory?

- Captures and compensates unknown pump-induced phase shifts
- Ensures physically consistent phase alignment across modes—key for coherent protocols (e.g. cluster states, error correction)
- The optimal global quadrature basis reveals maximal two-mode squeezing and graph structure

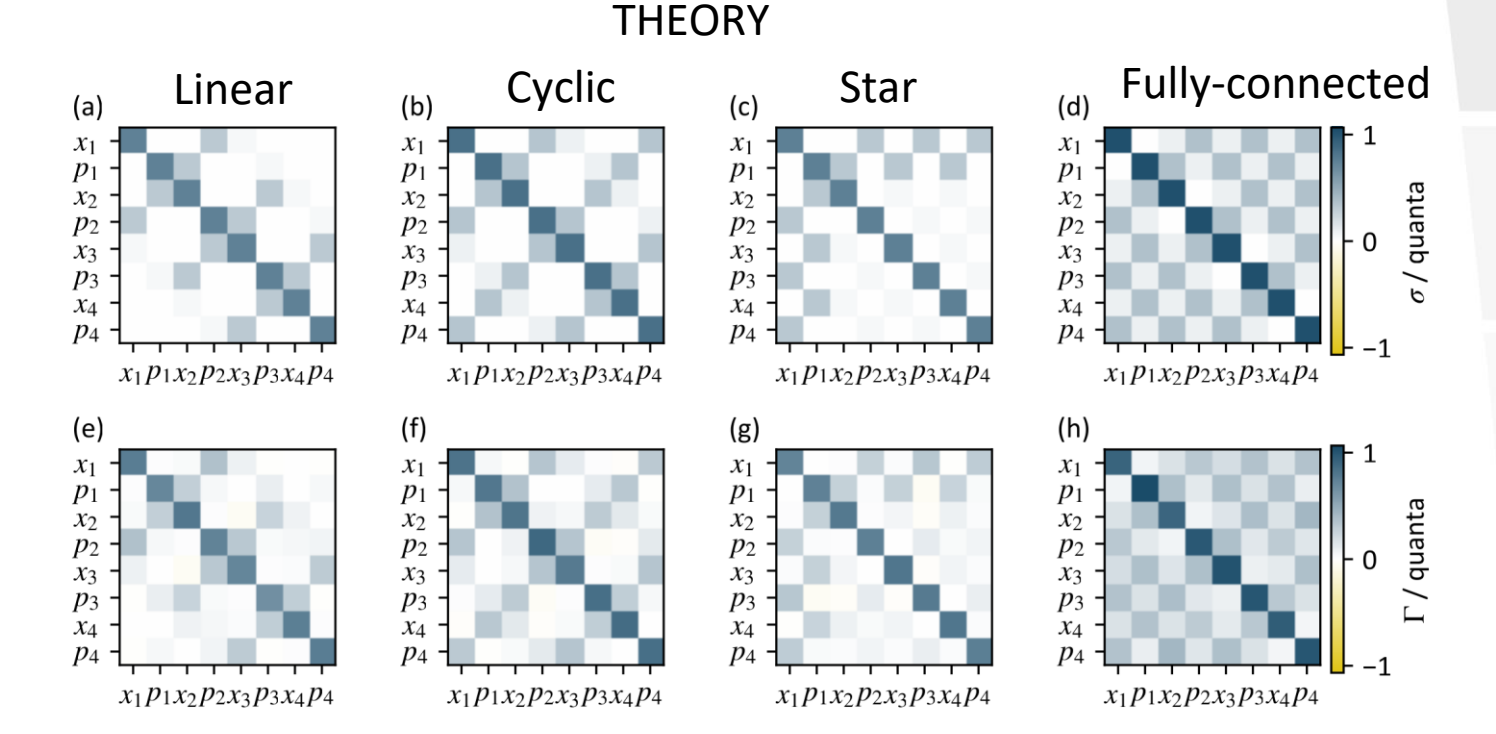




Comparison with Theory

- The reconstructed covariance matrix Γ is compared to its theoretical model σ
- The Frobenius distance quantifies the similarity between the two

$$\widetilde{\mathscr{F}}_{\mathrm{F}}(\sigma,\Gamma) = \exp\left(-\frac{\|\sigma - \Gamma\|_{\mathrm{F}}^2}{\|\sigma\|_{\mathrm{F}}^2}\right)$$



MEASUREMENT

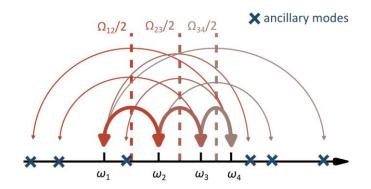


Role of Ancillary Modes: e.g. Linear CS

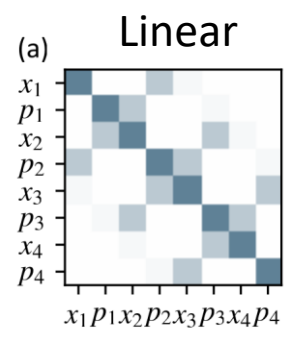
- Principal modes: 1–4 connected linearly via TMS links

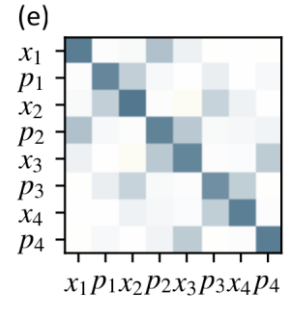
 (1,2),(2,3),(3,4)
- Ancillary modes: 5–10, connected to the principal chain via TMS links:

 (1,5), (1,6), (2,7), (3,8), (4,9), (4,10).



THEORY





MEASUREMENT

Generalized input-output relations

$$\hat{a}_{\mathrm{out},i} = \sum_{j} \left(\mathbf{U}_{ij} a_i + \mathbf{V}_{ij} \hat{a}_j^{\dagger} \right)$$

Bogoliubov matrices

$$\mathbf{U} = \mathbb{I}_m + (\cosh|r|-1) \cdot \operatorname{diag}(\mathbf{D}), \quad \mathbf{V} = \sinh|r| \cdot \mathbf{A}$$

Covariance matrix within symplectic formalism

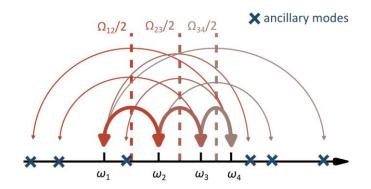
$$\boldsymbol{\sigma} = \frac{1}{2} \mathbf{S}_X \mathbf{S}_X^{\top} = \frac{1}{2} \begin{pmatrix} (\mathbf{U} + \mathbf{V})^2 & 0 \\ 0 & (\mathbf{U} - \mathbf{V})^2 \end{pmatrix}$$



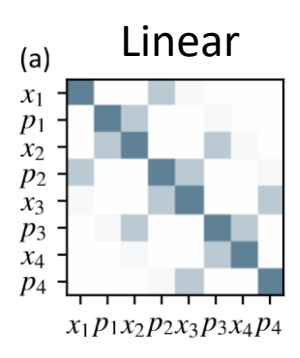
Role of Ancillary Modes: e.g. Linear CS

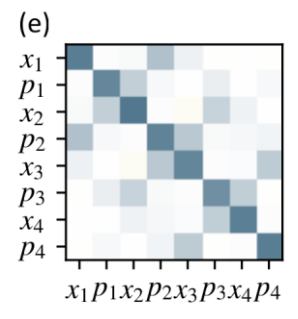
- Principal modes: 1–4 connected linearly via TMS links
 (1,2),(2,3),(3,4)
- Ancillary modes: 5–10, connected to the principal chain via TMS links:

 (1,5), (1,6), (2,7), (3,8), (4,9), (4,10).



THEORY





MEASUREMENT

Principal

Ancillary

$$\sigma_{\text{red}}^{(1:4)} = \begin{bmatrix} D & 0 & 0 & A & E & 0 & 0 & 0 \\ 0 & D & A & 0 & 0 & E & 0 & 0 \\ 0 & A & D & 0 & 0 & A & E & 0 \\ A & 0 & 0 & D & A & 0 & 0 & E \\ E & 0 & 0 & A & D & 0 & 0 & A \\ 0 & E & A & 0 & 0 & D & A & 0 \\ 0 & 0 & E & 0 & 0 & A & D & 0 \\ 0 & 0 & E & A & 0 & 0 & D \end{bmatrix}$$

•••

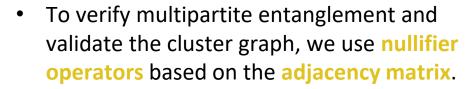
$$D = -6\cosh(|r|) + 3\cosh(2|r|) + \frac{7}{2}$$

$$A = (3\cosh(|r|) - 2)\sinh(|r|),$$

$$E = \frac{1}{2}\sinh^2(|r|).$$



Validation via Nullifier Measurements



$$\hat{\delta}_j = \hat{p}_j - \sum_{l=1}^m A_{jl} \hat{x}_l, \qquad j = 1, \dots, m$$

$$\hat{\boldsymbol{\delta}} = \mathbf{N} \cdot \hat{\boldsymbol{X}}, \quad \text{with} \quad \mathbf{N} = (-\mathbf{A} \mid \mathbb{I}_m)$$

Nullifier covariance matrix

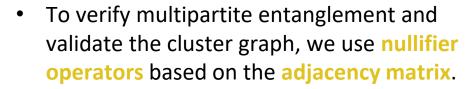
$$oldsymbol{\Delta} = \mathbf{N} oldsymbol{\sigma} \mathbf{N}^{ op}$$

Diagonal elements

$$\Delta_{jj} = \langle \hat{\delta}_j^2 \rangle - \langle \hat{\delta}_j \rangle^2 = \operatorname{Var}(\hat{\delta}_j)$$



Validation via Nullifier Measurements



$$\hat{\delta}_j = \hat{p}_j - \sum_{l=1}^m A_{jl} \hat{x}_l, \qquad j = 1, \dots, m$$

 In an ideal cluster state, nullifiers vanish; in practice, finite squeezing leads to small but nonzero variances.

$$\hat{\boldsymbol{\delta}} = \mathbf{N} \cdot \hat{\boldsymbol{X}}, \quad \text{with} \quad \mathbf{N} = (-\mathbf{A} \mid \mathbb{I}_m)$$

Nullifier covariance matrix

$$oldsymbol{\Delta} = \mathbf{N} oldsymbol{\sigma} \mathbf{N}^{ op}$$

Diagonal elements

$$\Delta_{jj} = \langle \hat{\delta}_j^2 \rangle - \langle \hat{\delta}_j \rangle^2 = \operatorname{Var}(\hat{\delta}_j)$$

Eg. 3-modes Cyclic cluster state

$$\mathbf{A} = \begin{pmatrix} 0 & 1 & 1 \\ 1 & 0 & 1 \\ 1 & 1 & 0 \end{pmatrix} \qquad \qquad \hat{\delta}_1 = \hat{p}_1 - \hat{x}_2 - \hat{x}_3 \\ \hat{\delta}_2 = \hat{p}_2 - \hat{x}_1 - \hat{x}_3 \\ \hat{\delta}_3 = \hat{p}_3 - \hat{x}_1 - \hat{x}_2$$



Validation via Nullifier Measurements

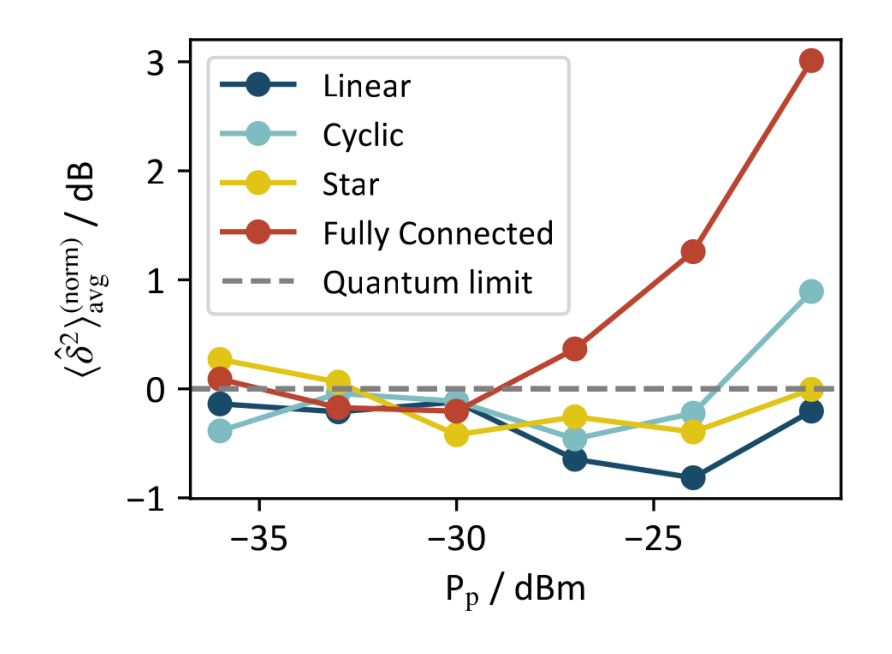
 To verify multipartite entanglement and validate the cluster graph, we use nullifier operators based on the adjacency matrix.

$$\hat{\delta}_j = \hat{p}_j - \sum_{l=1}^m A_{jl} \hat{x}_l, \qquad j = 1, \dots, m$$

- In an ideal cluster state, nullifiers vanish; in practice, finite squeezing leads to small but nonzero variances.
- A state is identified as a cluster state if all nullifier variances are below the shot noise level (vacuum limit).

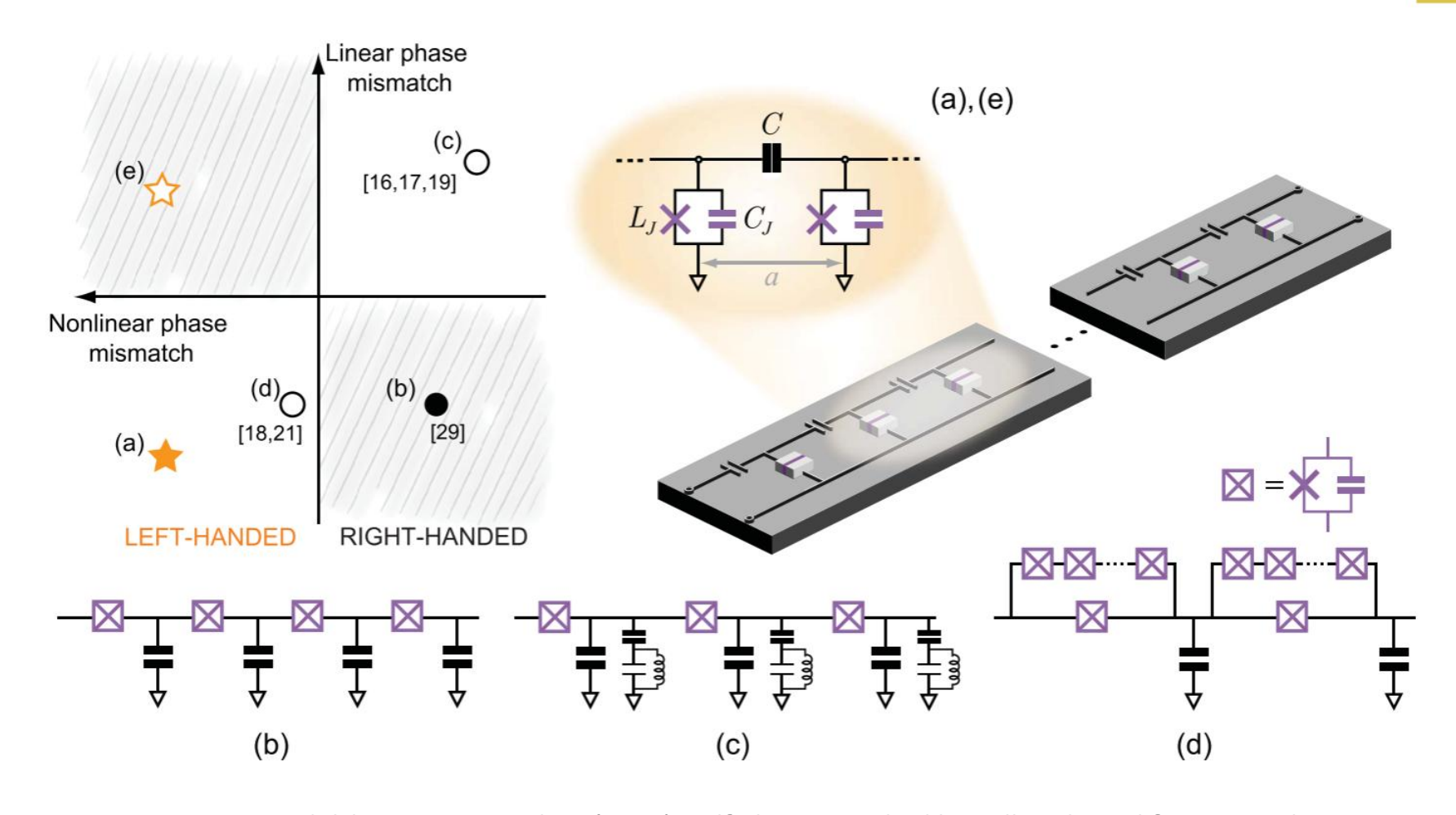
$$\langle \hat{\delta}_{j}^{2} \rangle = \langle \hat{p}_{j}^{2} \rangle + \sum_{l} A_{jl}^{2} \langle \hat{x}_{l}^{2} \rangle = \frac{1}{2} \left(1 + \sum_{l} A_{jl}^{2} \right)$$

$$\langle \hat{\delta}^{2} \rangle_{\text{avg}}^{(\text{norm})} = \frac{1}{m} \sum_{i=1}^{m} \frac{2\Delta_{jj}}{1 + \sum_{l} A_{jl}^{2}}$$





Squeezing-Gain trade-off



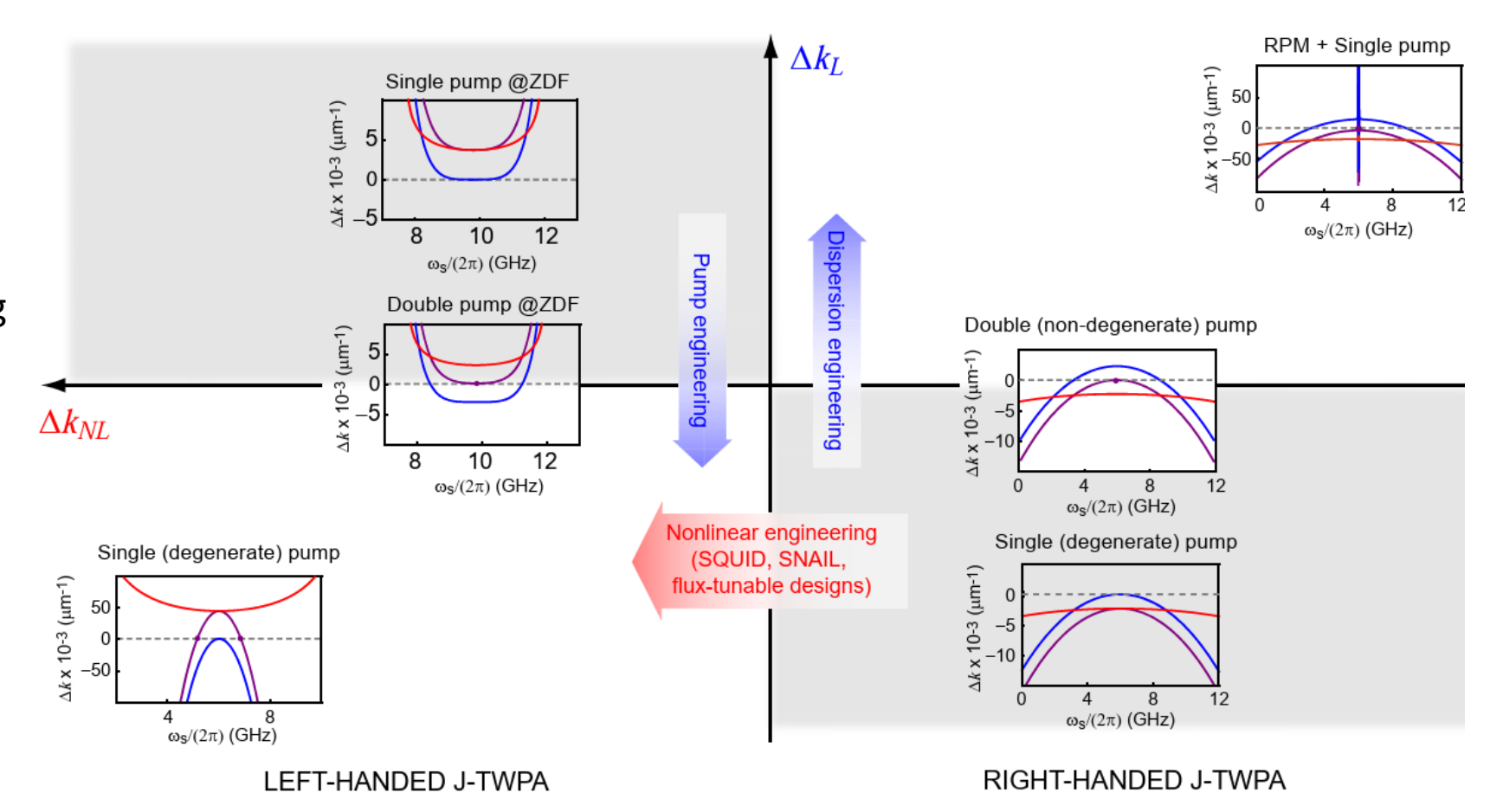
Kow, C., Podolskiy, V., & Kamal, A. (2024). Self phase-matched broadband amplification with a *left-handed Josephson transmission line*. http://arxiv.org/abs/2201.04660



Squeezing-Gain trade-off

Recall on the squeezing parameter

$$r_{jl}^{(k)} = g_{jl}^{(k)} \alpha_k e^{-i\phi_k}$$

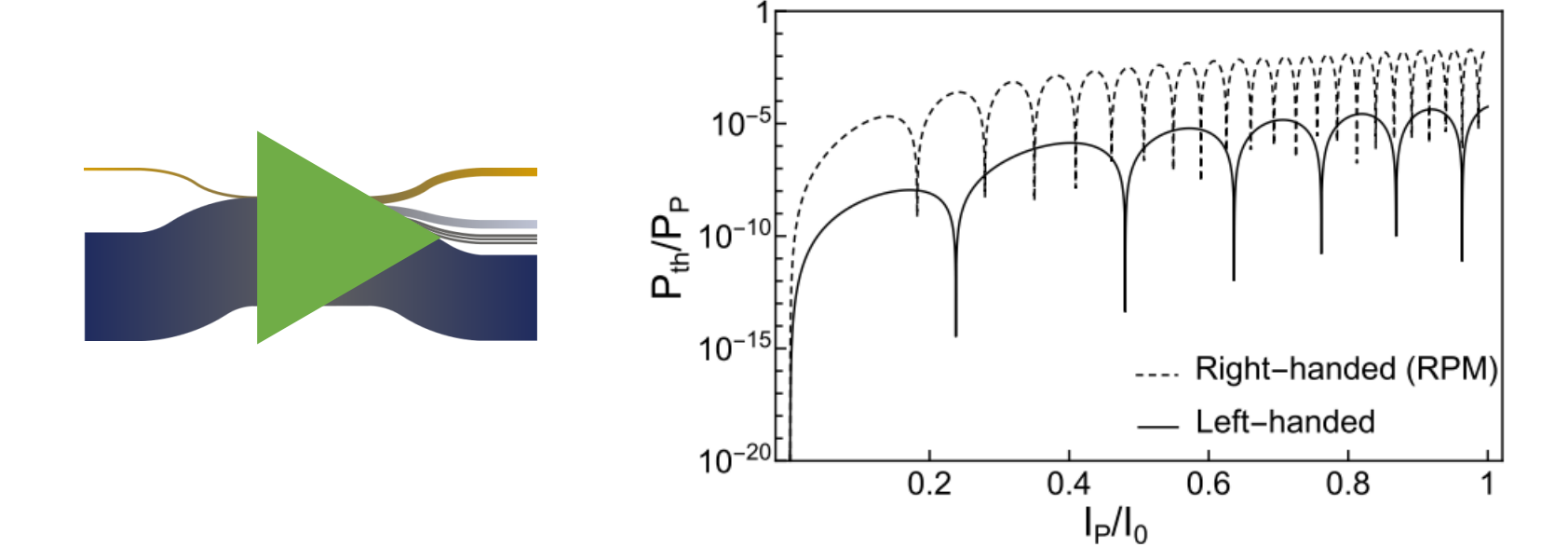


Kow, C., Podolskiy, V., & Kamal, A. (2024). Self phase-matched broadband amplification with a *left-handed Josephson transmission line*. http://arxiv.org/abs/2201.04660



Squeezing-Gain trade-off

Pump harmonics (and relative sidebands) dilute entanglement over multiple modes and increase complexity



Kow, C., Podolskiy, V., & Kamal, A. (2024). Self phase-matched broadband amplification with a *left-handed Josephson transmission line*. http://arxiv.org/abs/2201.04660

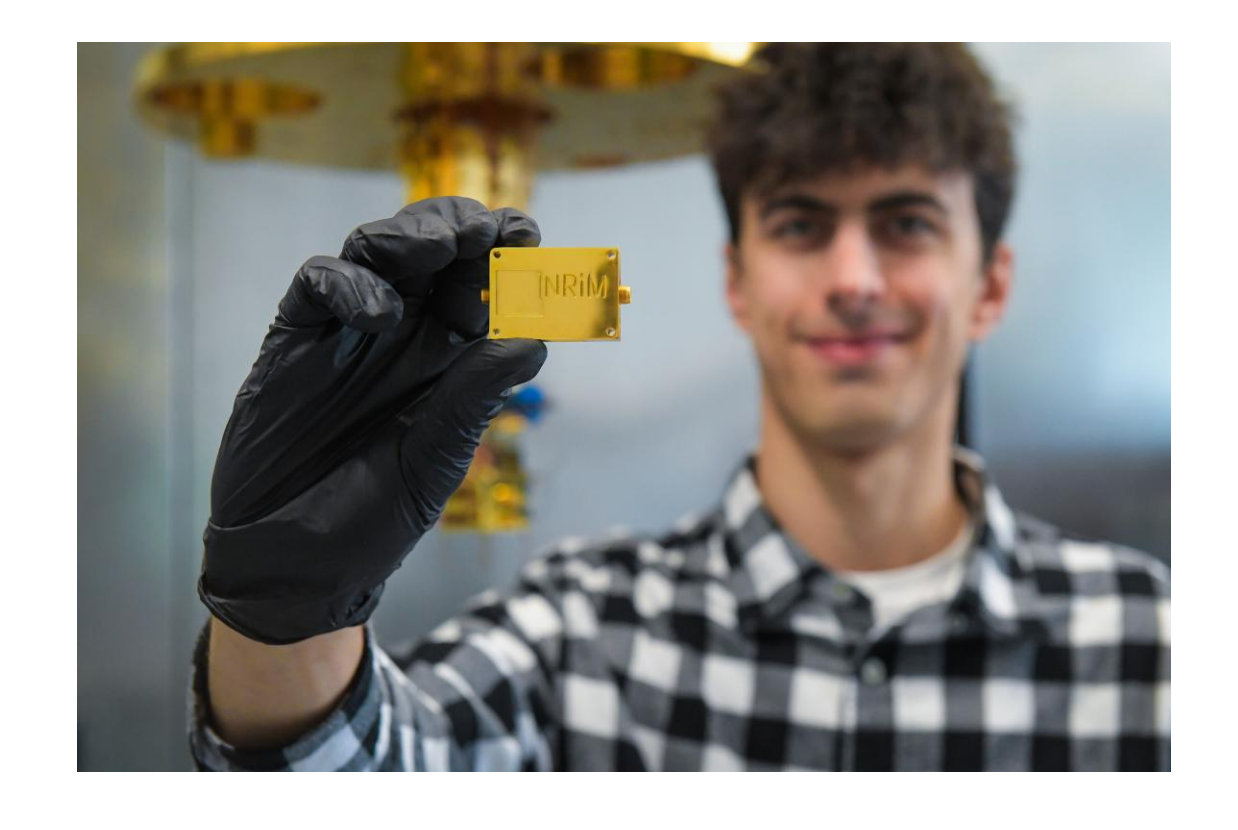


Conclusions and Perspectives

- We demonstrate a reconfigurable, scalable platform for generating continuous-variable cluster states using programmable pump engineering in a superconducting Josephson Travelling Wave Parametric Amplifier.
- Our method leverages the frequency domain to create large entangled graphs with minimal hardware overhead.
- Graph structure and entanglement are validated via nullifier measurements and covariance-based reconstruction.
- This approach bridges optical CV techniques and microwave superconducting hardware, enabling hardware-efficient measurement-based quantum computation.
- Future integration with LH-TWPAs and feedback could enable quantum algorithm execution.







Thanks for your attention!



Acknowledgments



























